

21 OCT. 1964

# INSTITUTE FOR AEROSPACE STUDIES

UNIVERSITY OF TORONTO

PERFORMANCE, OPERATION AND USE OF LOW ASPECT RATIO  
JET FLAPPED WINGS

by

G. K. Korbacher

TECHNISCHE HOOGESCHOOL DELFT  
Vliegtuigbouwkunde  
Michiel de Ruyterweg 10 - DELFT



MAY, 1964

UTIAS REPORT NO. 97

PERFORMANCE, OPERATION AND USE OF LOW ASPECT RATIO  
JET FLAPPED WINGS

by

G. K. Korbacher

MAY, 1964

UTIAS REPORT NO. 97

## ACKNOWLEDGEMENT

The author would like to thank Dr. G. N. Patterson, Director of the Institute, for providing the opportunity to work on this problem.

This work was supported by the U. S. Army - TRECOM, Task 1D121401A14203, Grant No. DA AMC-44-177-63-G9.

## SUMMARY

The characteristics of a jet flapped wing of aspect ratio 6 are presented, discussed and evaluated for STOL application.

Again, as for high aspect ratio ( $AR = 20$ ) jet flapped wings, a range for most economical jet flap operation is well defined. The angle of attack as an efficient means of lift production loses its usefulness with low aspect ratio jet flapped wings, whereas the optimum jet deflection angle seems hardly affected ( $\theta \approx 55^\circ$ ). A most efficient jet flap application for STOL calls for a complete integration of the lifting and propulsive systems.

In the range of most economical jet flap operation, semi-empirical relationships predict parameter changes accurately enough for practical purposes.

## TABLE OF CONTENTS

	<u>Page</u>
NOTATION	v
I. INTRODUCTION	1
II. DISCUSSION OF THE AVAILABLE EXPERIMENTAL DATA	1
III. THE LOW-ASPECT-RATIO JET-FLAPPED WING AT ZERO ANGLE OF ATTACK	2
3.1 Qualitative Jet Flap Characteristics	2
3.2 The Total Drag as a Function of $\Delta C_{LT}$	4
3.3 The "Constructed" Jet Flap Characteristics	5
3.4 The "Constant" $C_1$ and $K$	6
3.5 Effect of Aspect Ratio on $C_1$	6
3.6 The "Constant" $K$	7
3.7 The $d(\Delta C_{DT})/d(\Delta C_{LT}^2) = \text{Constant}$ Relationship	8
IV. THE LOW-ASPECT-RATIO JET-FLAPPED WING AT ANGLES OF ATTACK	9
4.1 Test Data Evaluation	9
4.1.1 $\theta = 37^\circ; 0^\circ \leq \alpha \leq 12^\circ$	9
4.1.2 $\theta = 67^\circ; 0^\circ \leq \alpha \leq 12^\circ$	10
4.2 The Jet Flap Characteristics	10
V. PERFORMANCE AND JET FLAP OPERATION	11
5.1 Jet Flap Performance	11
5.2 Most Economical Jet-Flap Operation	12
5.3 The Jet-Flapped Wing and STOL	14
5.4 Integration of the Lifting and Propulsive Systems	16
5.5 Wind Tunnel Testing of Jet-Flapped Wings	17
REFERENCES	18
FIGURES	

## NOTATION

AR	aspect ratio
$C_{\mu}$	jet momentum coefficient ( $= J/q S_w$ )
J	jet momentum ( $= M \cdot V_J$ )
M	jet mass flow
$V_J$	jet flow velocity
$V_{T1}$	take-off velocity of jet flap aircraft
$V_T$	take-off velocity of conventional aircraft
$S_w$	gross wing area
$\theta$	jet deflection angle
$\alpha$	angle of attack
$C_{\mu R}$	jet momentum coefficient, based on measured jet momentum
$C'_1$	a constant
$C_1$	a constant (see Eq. 3.3)
$C_D$	drag coefficient of wing without blowing
$C_{DT}$	total drag coefficient of jet flapped wing
$\Delta C_{DT}$	change in total drag coefficient due to blowing
$C_{LT}$	total lift coefficient of jet flapped wing
$\Delta C_{LT}$	change in total lift coefficient due to blowing
$C_{TM}$	total measured thrust coefficient as measured with a balance
$\Delta C_{TM}$	change in total thrust coefficient due to blowing
$\Delta C_{D_i}$	change in induced drag due to blowing
$\Delta C'_{D_i}$	change in induced drag due to $\Delta C_{LT}^2$ and AR

$\Delta C_{D_i}''$	change in induced drag due to $\Delta C_{LT}^2$ and $C_{\mu R}$
K	a constant (see Eq. 3.5)
K'	a constant (see Eq. 3.1)
K''	a constant (see Eq. 3.6)
K'''	a constant (= $1/\pi AR$ )
K'v	a constant (see Eq. 3.8)
$\Delta C_{DP}$	change in profile drag coefficient due to blowing (= $C_{DJ}$ )
$a(\theta)$	drag parameter, a function of $\theta$
$a(\alpha)$	drag parameter, a function of $\alpha$
$\Delta C_{DT_0}$	change in total drag, if $\Delta C_{D_i}''$ is ignored (see Eq. 3.9)
$C_2$	a constant (see Eq. 4.3)
$a(0)$	drag parameter for $\alpha = 0$
$C(x)$	drag parameter, a function of undefined quantity
$C_{\mu L}$	jet momentum coefficient, based on the rate of blowing required for production of the desired lift
$C_{\mu E}$	jet momentum coefficient, based on the entire jet engine exhaust.
$C_{\mu T}, C_{\mu C}$	jet momentum coefficients at take-off and cruise respectively of conventional aircraft
x	take-off distance of a specified conventional aircraft
$\rho$	air density

## I. INTRODUCTION

In Reference 1, characteristics of truly and quasi two-dimensional jet-flapped wings are presented; in addition, jet-flap performance, economy of operation, application to STOL aircraft, are discussed. Three "constants" were found to dominate that portion of the characteristics which confines the range of most economical jet-flap operation. Naturally, in this range, any increment in the rate of flap blowing is completely (100%) recovered as (balance) measured thrust.

In operational applications for STOL aircraft, for example, two-dimensional jet-flap results are of rather academical value. The effect of aspect ratio on the economy of lift production is crucial, and the drag penalty commensurate with high lift producing, low-aspect-ratio jet-flapped wings needs careful study and evaluation.

Unfortunately, there is only one set of test results of a low-aspect-ratio (AR = 6) jet-flapped wing available which is, however, not as complete as would be desirable for the unambiguous construction of its characteristics. It is this set of test data (Ref. 2) which is evaluated in this paper.

## II. DISCUSSION OF THE AVAILABLE EXPERIMENTAL DATA

In Ref. 2, the results of wind tunnel experiments with a rectangular jet-flapped wing of aspect ratio 6 are reported. These tests were primarily conducted with full-span blowing over a 10% chord jet control flap. At rates of blowing from zero to  $C_{\mu} = 2.3$ , the lift and thrust (drag) was measured at four jet sheet deflection angles ( $\theta = 0^{\circ}, 37^{\circ}, 67^{\circ},$  and  $97^{\circ}$ ) and at angles of attack,  $\alpha$ , ranging from  $-8^{\circ}$  to  $+20^{\circ}$ .

Unfortunately, these test results were obtained for a wing-body combination (with and without tail). The wing alone was not tested. Therefore, the presented lift and thrust (drag) values contain the body contributions to lift and thrust (drag).

In Ref. 2, it is the sectional momentum coefficient,  $C'_{\mu}$ , against which most of the presented data are plotted. In this paper, the overall momentum coefficient,  $C_{\mu} = 0.9 C'_{\mu}$ , related to the gross wing area (which corresponds to the spanwise extent of the blowing slot instead of the reference area excluding the body cutout) is used. Lift and thrust (drag) coefficients are also related to the gross wing area.

For the jet-sheet momentum from which  $C_{\mu}$  is obtained, the actual (real) jet momentum at the trailing edge of the jet control flap is used. In Ref. 2, a correction of 0.85 to the calculated jet sheet momentum is suggested, based on careful estimates of contributing factors. The real  $C_{\mu R}$  is then given by  $C_{\mu R} = 0.85 C_{\mu}$ .

The test data of Ref. 2 can be presented in two ways: either as balance measured lift and thrust (drag) values ( $C_{LT}$  and  $C_{TM}$  ( $C_{DT}$ ) respectively), or as  $\Delta C_{LT}$  and  $\Delta C_{TM}$  ( $\Delta C_{DT}$ ) values. The  $\Delta$  designates the increments in lift or thrust (drag) due to blowing. For design purposes, the overall (balance) measured values should be more informative. For an analysis of the jet flap, however, values which are unobscured by the lift and drag of the basic wing, alone or in combination with either a shrouded jet flap or a jet control flap, are preferable. Moreover, on the basis of  $\Delta$  values, various jet-flap configurations can be compared with the pure jet flap as to how efficiently a given amount of jet momentum can produce lift and thrust (drag). In this paper, primarily  $\Delta$  values are used.

### III. THE LOW-ASPECT-RATIO JET-FLAPPED WING AT ZERO ANGLE OF ATTACK

#### 3.1 Qualitative Jet Flap Characteristics

If the converted jet flap data of Ref. 2 for the full-span blowing wing-body combination (without tail) are evaluated, the balance measured thrust due to blowing,  $\Delta C_{TM}$ , can be plotted versus  $C_{\mu R}$  for various jet sheet deflection angles  $\theta$  (see Fig. 1). This plot does not yet constitute a jet flap characteristics. The  $\Delta C_{LT} = \text{constant}$  lines still have to be added. Unfortunately, the test data of Ref. 2 are not comprehensive enough to do this unambiguously. For instance, there are not sufficient test points available to define either the direction of the straight portions of the  $\Delta C_{LT} = 1, 1.5, 2, 2.5,$  and  $3$  lines or the location and direction of the  $\Delta C_{LT} = 4$  and  $5$  lines. This is the reason why - as a first approximation - the straight portions of the  $\Delta C_{LT} = \text{constant}$  lines are drawn as lines parallel to the 100% thrust recovery slope line. This approximation was chosen on account of two observations:

- a) that  $\Delta C_{LT} = \text{constant}$  lines are parallel to the 100% thrust recovery slope line if the aspect ratio of the jet-flapped wing is large or infinite (see Ref. 1).
- b) that the change of induced drag,  $\Delta C_{Di}$ , with rate of blowing  $C_{\mu R}$  (which is the only reason for an inclination of the  $\Delta C_{LT} = \text{constant}$  lines with the 100% thrust recovery slope line), is small, at least for the  $AR = 6$  jet-flapped wing under consideration here.

Drawing the  $\Delta C_{LT} = \text{constant}$  lines through the corresponding test points of the  $\theta = 37^\circ$  curve leads to the qualitative jet flap characteristics presented in Fig. 1. The  $\Delta C_{LT} = 4$  and  $5$  lines are lines through points A and B respectively, where A and B were calculated (assuming that the  $\theta = 37^\circ$  curve is a straight line, which it is not) from

$$\Delta C_{DT} = \frac{C'_1}{K'^2} \cdot \Delta C_{LT}^2 \quad (3.1)$$

after  $C_1/K^2$  was obtained from  $\Delta C_{DT}/\Delta C_{LT}^2 = 0.47/6.25 = 0.0753$  at point C.

Comparing now Fig. 1 with characteristics of truly or quasi two-dimensional jet-flapped wings (see Figs. 10, 11 and 12 of Ref. 1), the effect of aspect ratio becomes quite apparent. The lines of  $\theta = \text{constant}$  fan out stronger, move closer to or even above the  $C_{\mu R}$  axis, and strongly depart from straight lines at higher values for  $\theta$ . The lines of  $\Delta C_{LT} = \text{constant}$  are further apart. Both observations reflect the expected appreciable total drag increase of low-aspect-ratio jet-flapped wings operated under high lift conditions.

Again, as in the high-aspect-ratio jet flap characteristics of Ref. 1, the  $\Delta C_{LT} = \text{constant}$  lines in Fig. 1 seem basically to be straight lines. Above the "operating line" (the locus of the points where the  $\Delta C_{LT} = \text{constant}$  lines depart from a straight line), operation of the jet-flapped wing at fixed  $\Delta C_{LT}$  can no longer be achieved (neglecting still the effect of  $C_{\mu R}$  on the induced drag) at a constant profile drag. The increase in profile (and total) drag ( $\delta \Delta C_{DP} = \delta \Delta C_{DT}$ ) with jet flap operation above the operating line is given by the horizontal distance between the extended straight  $\Delta C_{LT} = \text{constant}$  line and its real counterpart (see Fig. 1). The changes in blowing rate, thrust, and drag above the operating line are related (see Ref. 1) as

$$\delta(\Delta C_{TM}) = \delta C_{\mu R} - \delta(\Delta C_{DT}) \quad (3.2)$$

which for jet flap operation along or below the operating line (where  $\delta(\Delta C_{DT})$  is presently assumed to be zero) reduces to

$$\delta(\Delta C_{TM}) = \delta C_{\mu R}.$$

Also in Ref. 1, the following relationships were derived for truly and quasi two-dimensional jet-flapped wings:

$$\Delta C_{DT} = a(\theta) C_{\mu R} = C_1 \sin^2 \theta C_{\mu R} \quad (3.3)$$

and

$$\Delta C_{DT} = \frac{C_1}{K^2} \cdot \Delta C_{LT}^2 \quad (3.4)$$

Equation 3.4 is obtained when Eq. 3.3 is combined with Spence's expression (Ref. 3).

$$\Delta C_{LT}^2 = K^2 \sin^2 \theta C_{\mu R} \quad (3.5)$$

where K is a characteristic "constant" of the jet flap configuration in question.

In subsequent sections of this paper, the effect of induced drag on jet flap characteristics as a whole and on "constants" such as  $C_1$ ,  $K$ , and  $K''$  in particular will be considered.

### 3.2 The Total Drag as a Function of $\Delta C_{LT}$

For spanwise elliptic loading, the total drag of jet-flapped wings due to blowing can be obtained from

$$\begin{aligned} \Delta C_{DT} &= K'' \cdot \Delta C_{LT}^2 + \Delta C_{Di} \\ &= K'' \Delta C_{LT}^2 + \frac{\Delta C_{LT}^2}{\pi AR(1 + 2C_{\mu R}/\pi AR)} \end{aligned} \quad (3.6)$$

For truly two-dimensional jet flaps,  $\Delta C_{Di} = 0$ ; for quasi two-dimensional jet-flapped wings, the effect of  $C_{\mu R}$  on the induced drag is small enough to be neglected, and

$$\begin{aligned} \Delta C_{DT} &= K'' \cdot \Delta C_{LT}^2 + \frac{\Delta C_{LT}^2}{\pi AR} \\ &= (K'' + K''') \Delta C_{LT}^2 = \Delta C_{DT0} \end{aligned} \quad (3.7)$$

if  $K'''$  is substituted for  $1/\pi AR$ . For low-aspect-ratio wings, the effect of  $C_{\mu}$  on the induced drag can no longer be ignored. To demonstrate this point, the induced drag  $\Delta C_{Di}$  is plotted in Fig. 2 versus  $C_{\mu R}$ , for various values of  $\Delta C_{LT} = \text{constant}$  and for two aspect ratios,  $AR = 6$  and  $3$ . It is quite obvious that, at least for aspect ratios of  $6$ , the change in  $\Delta C_{Di}$  with  $C_{\mu R}$  (at  $\Delta C_{LT} = \text{constant}$ ) can for all practical purposes be represented by a linear function. For the  $AR = 3$  wing this seems to be possible only for lift values of  $\Delta C_{LT} < 3$ . If, nevertheless, we approximate also the  $\Delta C_{LT} = 4$  and  $5$  lines in Figure 2 ( $AR = 3$ ) by straight lines as shown, determine the slopes of all  $\Delta C_{LT} = \text{constant}$  lines, and plot them versus  $\Delta C_{LT}^2$ , Fig. 3 results. It indicates that the change in  $\Delta C_{Di}$  due to blowing can be expressed as

$$\begin{aligned} d \Delta C_{Di} / d C_{\mu R} &= \text{constant} \cdot \Delta C_{LT}^2 \\ &= K'^V \cdot \Delta C_{LT}^2 \end{aligned} \quad (3.8)$$

where  $K'^V = 0.00464$  or  $0.0158$  for the  $AR = 6$  and  $3$  jet-flapped wings respectively. In other words, the total drag of a low-aspect-ratio jet-flapped wing can, at least so long as its aspect ratio is not much below  $6$ , be obtained for all practical purposes from

$$\begin{aligned} \Delta C_{DT} &= (K'' + K''') \Delta C_{LT}^2 - K'^V \cdot \Delta C_{LT}^2 C_{\mu R} \\ &= \Delta C_{DT0} - \Delta C_{Di}'' \end{aligned} \quad (3.9)$$

Here,  $\Delta C_{DT_0}$  is the sum of the profile drag ( $\Delta C_{DP} = K'' \Delta C_{LT}^2$ ) and the induced drag ( $\Delta C_{Di} = K''' \Delta C_{LT}^2$ ), assuming that the lift  $\Delta C_{LT}$  is produced without blowing ( $C_{\mu R} = 0$ ). In case of nonelliptical spanwise wing loading, the constants  $K'''$  and  $K''$  would have to be multiplied by a factor which accounts for the actual wing loading.

### 3.3 The "Constructed" Jet Flap Characteristics

Because of the lack of test points for the AR = 6 jet-flapped wing of Ref. 2, an attempt is made to construct its characteristics by supplementing the original test data of Ref. 2 with the help of semiempirical relationships derived from the experimental evidence.

The characteristics presented in Fig. 1 were obtained under the inappropriate assumption that the  $\Delta C_{LT} = \text{constant}$  lines are also lines of  $\Delta C_{DT} = \text{constant}$  and therefore parallel to the 100% thrust recovery slope line. We have seen, however, that along the  $\Delta C_{LT} = \text{constant}$  lines, the total drag  $\Delta C_{DT} \neq \text{constant}$ , but changes according to Eq. 3.9. Assuming now (and this assumption is established reasonably well) that the profile drag of jet-flapped wings ( $\Delta C_{DP} = K'' \Delta C_{LT}^2$ ) does not change at fixed  $\Delta C_{LT}$  and small jet deflection angles (say  $\theta < 50^\circ$ ), Eq. 3.9 can be used to calculate  $\Delta C_{DT_0}$  from

$$\Delta C_{DT_0} = \Delta C_{DT} + \Delta C_{Di}''.$$

If we plot again the converted test data of Ref. 2 for the  $\theta = 37^\circ$ ,  $67^\circ$ , and  $97^\circ$  parameter, point A in Fig. 4 would then define the thrust ( $\Delta C_{TM}$ ), the total drag ( $\Delta C_{DT}$ ), and the rate of blowing commensurate with a  $\Delta C_{LT} = 2.5$  at  $\theta = 37^\circ$ . If now  $\Delta C_{Di}''$ , as calculated from

$$\Delta C_{Di}'' = K'''. \Delta C_{LT}^2 C_{\mu R}, \quad (3.10)$$

is added to  $\Delta C_{DT}$  at point A, point B is obtained. If through B, a line parallel to the 100% thrust recovery slope line is drawn, this line would represent the locus of  $\Delta C_{LT} = 2.5$  for an AR = 6 jet-flapped wing, the induced drag of which would be independent of the rate of blowing. Where this line intersects the vertical axis (point C),  $\Delta C_{DT_0} = \Delta C_{DT}$  since  $\Delta C_{Di} = 0$  on account of zero blowing ( $C_{\mu R} = 0$ ). If point C is connected with A by a straight line, this line should represent the real  $\Delta C_{LT} = 2.5$  line so long as the profile drag does not change or  $\Delta C_{DT_0} = \text{constant}$ .

The above procedure, repeated for points D, E, etc., should furnish the real  $\Delta C_{LT} = 3.0, 2.0, 1.5,$  and  $1.0$  lines. A simpler way, however, is to find the points F, G, etc., from the relationship

$$\begin{aligned} \Delta C_{DT_0} &= \text{constant} \cdot \Delta C_{LT}^2 \\ &= (K'' + K''') \cdot \Delta C_{LT}^2 \end{aligned} \quad (3.11)$$

Here  $(K'' + K''')$  can be obtained from point C as

$$(K'' + K''') = \frac{\Delta C_{DT_0}}{\Delta C_{LT}^2} = \frac{0.52}{6.25} = 0.0833$$

and we get for

$\Delta C_{LT}$	=	1.0	1.5	2.0	2.5	3	4	5
$\Delta C_{DT_0}$	=	0.0833	0.1875	0.333	0.52	0.75	1.333	2.083

There is some complication in finding the location of the real  $\Delta C_{LT} = 4$  line. At an angle  $\theta = 67^\circ$ , it seems evident (see operating line) that the  $\Delta C_{LT} = \text{constant}$  lines have already deviated from a straight line. This evidence suggests that the  $\Delta C_{LT} = 4$  line cannot be drawn as a straight line through L and J. If, however, we calculate  $\Delta C_{D_i}''$  at point J from

$$\begin{aligned} \Delta C_{D_i}'' &= K^{1v} \cdot \Delta C_{LT}^2 C_{\mu R} \\ &= 0.00464 \times 16 \times 1.24 = 0.092 \end{aligned} \quad (3.10)$$

and subtract 0.092 from the  $\Delta C_{DT_0} = 1.333$  at point H, we obtain point K, through which the real  $\Delta C_{LT} = 4$  line should run, provided it would be still straight at  $\theta = 67^\circ$ . Since point J is above K, this can not be the case and the  $\Delta C_{LT} = 4$  line must have already departed from a straight line at an angle  $\theta < 67^\circ$ .

### 3.4 The "Constant" $C_1$ and K

For truly and quasi two-dimensional jet flapped wings (see Ref. 1), the relationship

$$\Delta C_{DT} = \frac{C_1}{K^2} \cdot \Delta C_{LT}^2 \quad (3.4)$$

was shown to apply along or below the operating line. In this regime, the  $\Delta C_{LT} = \text{constant}$  lines were straight and parallel to the 100% thrust recovery slope line and both  $C_1$  and K were true constants. Let us now consider the effect of aspect ratio on  $C_1$  and K.

### 3.5 Effect of Aspect Ratio on $C_1$

If  $\Delta C_{DT}$  is plotted versus  $C_{\mu R}$  with the jet sheet deflection angle  $\theta$  as the parameter, the solid lines in Fig. 5 are obtained. It is quite obvious that the straight line relationship

$$\Delta C_{DT} = a(\theta) C_{\mu R} \quad (3.3)$$

(found to apply for truly and quasi two-dimensional jet-flapped wings, see Ref. 1) no longer applies at large jet deflection angles and only approximates

the test data at small  $\theta$  values ( $\theta \leq 37^\circ$ ). Theoretically, the drag parameter

$$a(\theta) = C'_1 \sin^2\theta$$

is no longer a function of  $\theta$  alone and the "constant"  $C'_1$  is no longer a constant even when the jet-flapped wing is operated below the operating line. In this regime, the profile drag does not change, but the induced drag decreases with increasing  $C_{\mu R}$ . If one calculates the induced drag contribution due to blowing,  $\Delta C_{D_i}''$ , from Eq. 3.10 for the test points of the  $\theta = 37^\circ$ ,  $67^\circ$ , and  $97^\circ$  curves in Fig. 5 and thus adds the obtained values at the test points, the lines

$$\Delta C_{DT_0} = \Delta C_{DT} + \Delta C_{D_i}''$$

are obtained. These lines should be straight so long as  $C_1$  is a constant. The  $\Delta C_{DT_0}$  line for  $\theta = 37^\circ$  is straight, but those for  $\theta = 67^\circ$  and  $97^\circ$  are only approximately straight lines.

If Eqs. 3.4 and 3.9 are combined,  $C'_1$  can be obtained from

$$\Delta C_{DT} = \frac{C'_1}{K'^2} \cdot \Delta C_{LT}^2 = \frac{C_1}{K^2} \cdot \Delta C_{LT}^2 - K'^v \cdot \Delta C_{LT}^2 C_{\mu R} \quad (3.12)$$

as

$$C'_1 = C_1 - K^2 K'^v C_{\mu R} \quad (3.13)$$

assuming that  $K' = K$ .  $C'_1$  is plotted in Fig. 6. The "constant"  $C_1$  is a true constant as long as  $\Delta C_{DT_0}$  at fixed  $\Delta C_{LT}$  is constant and can be determined either from

$$C_1 = K^2 (K'' + K''') \quad (3.14)$$

or from

$$C_1 = K^2 \frac{\Delta C_{DT_0}}{\Delta C_{LT}^2} \quad (3.15)$$

If one plots the slope  $a(\theta) = d \Delta C_{DT} / d C_{\mu R}$  of the  $\theta = 37^\circ$  line and the approximated slopes of the  $\theta = 67^\circ$  and  $97^\circ$  curves versus  $\sin^2\theta$ , Fig. 7 results. Added in this figure are the slope  $d \Delta C_{DT_0} / d C_{\mu R}$  for  $\theta = 37^\circ$  and, for comparison, the slopes obtained from the truly and quasi two-dimensional jet-flapped wings considered in Ref. 1. Again, from the viewpoint of completeness and conclusiveness of the presented evidence, it is very unfortunate that the test data for one more jet deflection angle of about  $50^\circ$  are not available for the  $AR = 6$  wing of Ref. 2.

### 3.6 The "Constant" K

This "constant" can be calculated from Eq. 3.5. It is plotted versus  $C_{\mu R}$  in Fig. 8, using either  $\theta$  or  $\Delta C_{LT}$  as the parameter.

A comparison of Fig. 8 with Fig. 13 of Ref. 1 demonstrates the effect of aspect ratio on K. Whereas for truly and quasi two-dimensional jet-flapped wings, K is equal to 4 for a pure jet flap and greater than 5 for jet control flaps with upper surface or symmetrical blowing, the K value for the aspect ratio AR = 6 jet-flapped wing under consideration (a jet control flap with upper surface blowing) is K = 3.15 as long as this wing is operated along or below the operating line. Above it, K becomes larger.

If, to experimentally prove or disprove Eq. 3.5 for low-aspect-ratio jet-flapped wings,  $\Delta C_{LT}^2$  is plotted against  $C_{\mu R}$  for fixed  $\theta$  values, Fig. 9 is obtained. Next, if the slopes  $b(\theta)$  of the  $\theta = \text{constant}$  curves are determined and plotted against  $\sin^2\theta$ , Fig. 10 results. Figure 10 suggests that Eq. 3.5 holds for jet deflection angles of up to approximately 50 degrees, the angle at which the  $\Delta C_{LT} = \text{constant}$  lines seem to depart from straight lines.

As previously indicated in the analysis of  $C'_1$ , tests with just one more jet deflection angle ( $\theta \approx 50^\circ$ ) in Ref. 2, also would have enhanced the conciseness and conclusiveness of the K data presented in Figs. 8 and 10.

### 3.7 The $d(\Delta C_{DT})/d(\Delta C_{LT}^2) = \text{Constant}$ Relationship

Since  $d(\Delta C_{DT})/d(\Delta C_{LT}^2) = C'_1/K^2$  and  $C'_1/K^2$  changes with  $C_{\mu R}$  as shown in Fig. 6, theoretically this relationship no longer holds. How valid it is in practice is considered below.

If in Fig. 4, the line A-A is drawn and the  $\Delta C_{DT}$  and  $\Delta C_{DT_0}$  values are read off for the points where line A-A intersects the  $\Delta C_{LT} = \text{constant}$  lines, the curves for  $\Delta C_{DT}$  and  $\Delta C_{DT_0}$  in Fig. 11 are obtained. The straight-line relationship for

$$d(\Delta C_{DT_0})/d(\Delta C_{LT}^2) = C_1/K^2$$

is expected, since both  $C_1$  and K appear to be constants provided that the jet-flapped wing is operated below the operating line. The  $\Delta C_{DT}$  curve can be approximated reasonably well by a straight line up to  $\Delta C_{LT}$  values of about 4. But the slope of this line ( $= C'_1/K^2$ ) does not mean much since it depends on where the A-A in Fig. 4 is drawn.

Further, in Fig. 11, the drag-lift relationship at constant jet deflection angle is shown for  $\theta = 37^\circ$ ,  $67^\circ$ , and  $97^\circ$ . The change of both  $C'_1$  and K with  $\theta$  is demonstrated. At  $\theta = 37^\circ$ , K for the  $C_{\mu R}$  range of practical jet flap operation can be considered as a constant for all jet deflection angles smaller than the one related to the operating line. Therefore it must be  $C'_1$  (actually  $\Delta C_{D_i}$ ) which causes the departure of the  $\theta = 37^\circ$  curve from a straight line. In the case of the  $\theta = 67^\circ$  curve, both  $C'_1$  and  $K^2$  increase, but their ratio is only little affected. At  $\theta = 97^\circ$ , the effect

of  $\Delta C_{D_i}$  diminishes (due to smaller rates of blowing) and the increase in profile drag dominates.

In conclusions, it can be said that at lower aspect ratios ( $AR \approx 3$ ), the linear relationship between the total drag and the lift, which is found to apply for wings of large aspect ratios ( $AR > 10$ ), no longer holds, even approximately.

#### IV. THE LOW-ASPECT-RATIO JET-FLAPPED WING AT ANGLES OF ATTACK

The test data of Ref. 2 demonstrate the variation of measured thrust and total lift for four jet deflection angles ( $\theta = 7^\circ, 37^\circ, 67^\circ$ , and  $97^\circ$ ) at various angles of attack ( $-8^\circ < \alpha < 16^\circ$ ).

As Fig. 4 demonstrates, operation of a jet-flapped wing at  $\theta = 7^\circ$  or  $\theta = 97^\circ$  is unwarranted. At  $\theta = 7^\circ$ , the rates of blowing required for the production of lift magnitudes, which would justify the use of a jet flap, are uneconomically high. At  $\theta = 97^\circ$ , the drag penalty for high lift operation is prohibitive. Since this paper is intended to deal primarily with the practical operation and performance of jet-flapped wings, subsequent considerations are restricted to operational jet deflection angles ( $\theta = 37^\circ$  and  $67^\circ$ ). Reference to the  $\theta = 7^\circ$  and  $97^\circ$  test data is made only where, basically or comparatively, these data are useful in the context of the presented material.

##### 4.1 Test Data Evaluation

The converted test data of Ref. 2 for  $\theta = 37^\circ$  and  $67^\circ$  at various angles of attack ( $\alpha$ ) are presented below.

##### 4.1.1 $\theta = 37^\circ; 0^\circ \leq \alpha \leq 12^\circ$

If we plot  $\Delta C_{DT}$  versus  $C_{\mu R}$  for various angles of attack, a family of straight lines is obtained. If the points of constant  $\Delta C_{LT}$  are connected, the plot of Fig. 12a results. Note that the  $\Delta C_{DT}$  lines at constant  $\alpha$  values are straight lines for all practical purposes (this would not occur at  $AR = 3$ , for instance, because of the larger  $\Delta C_{D_i}$ ). If the slopes,  $a(\alpha)$ , of the  $\Delta C_{DT}$  lines are plotted versus  $\sin^2 \alpha$ , Fig. 12b is obtained.

Figure 12 demonstrates that  $\Delta C_{DT}$  at fixed  $\theta = 37^\circ$  obeys the relationship

$$\Delta C_{DT} = a(\alpha) C_{\mu R} \quad (4.1)$$

and that

$$d [a(\alpha)] / d \sin^2 \alpha = C_2 = 6.2 \quad (4.2)$$

From Eq. 4.2 it follows that

$$a(\alpha) + C = C_2 \sin^2 \alpha \quad (4.3)$$

If all the straight  $\Delta C_{DT}$  lines in Fig. 12a would pass through the origin, the integration constant  $C$  would be simply the slope  $a(0)$  of the  $\Delta C_{DT}$  line for  $\alpha = 0$  (which also represents the  $\Delta C_{DT}$  line for  $\theta = 37^\circ$ ). Note that the actual  $\Delta C_{DT}$  lines must pass through the origin (a condition resulting from plotting  $\Delta C_{DT}$  instead of  $C_{DT}$ ). The constant  $C$  can then be expressed as

$$C = a(0) + C(x) = a(\theta) + C(x) \quad (4.4)$$

Since  $a(\theta) = a(0) = 0.27$  for  $\theta = 37^\circ$ ,  $C$  becomes

$$C = 0.27 + C(x)$$

and

$$\Delta C_{DT} = C(x) + (a(\theta) + C_2 \sin^2 \alpha) C_{\mu R} \quad (4.5)$$

where  $C(x)$  is an unknown function. Equation 4.5 can also be written as

$$\Delta C_{DT} = C(x) + (C'_1 \sin^2 \theta + C_2 \sin^2 \alpha) C_{\mu R} \quad (4.6)$$

This latter equation accounts for the fact that actually the  $\Delta C_{DT}$  line for  $\alpha = 0$  is theoretically not a straight line and due to  $\Delta C_{D_i}$  departs the more from a straight line, the lower the aspect ratio.

#### 4.1.2 $\theta = 67^\circ; 0^\circ \leq \alpha \leq 12^\circ$

If at  $\theta = 67^\circ$ ,  $\Delta C_{DT}$  versus  $C_{\mu R}$  is plotted for several fixed angles of attack, Fig. 13 is obtained, in which also the lines of constant  $\Delta C_{LT}$  are added.

Just as Fig. 5 previously demonstrated the inapplicability of Eq. 3.3 at large jet deflection angles, Fig. 13 illustrates the inapplicability of Eq. 4.1. It is to be expected that when the profile drag along the  $\Delta C_{LT} =$  constant lines is no longer constant, drag, lift, and drag-lift relationships can no longer be represented by simple linear functions.

## 4.2 The Jet Flap Characteristics

If in the characteristics presented in Fig. 4, the  $\Delta C_{LT} =$  constant lines obtained by varying  $C_{\mu R}$  and the angle of attack at fixed jet deflection angle are added, Fig. 14 results. Since the lines for  $\theta = 37^\circ$  and  $67^\circ$  are far enough apart, the  $\Delta C_{LT} =$  constant lines for changing  $\alpha$  can be shown in this figure for both  $\theta = 37^\circ$  and  $67^\circ$  without overcrowding the characteristics. The location of the operating line is rather vague since the points where the  $\Delta C_{LT} =$  constant lines depart from straight lines are difficult to define.

To facilitate comparison of Fig. 14 with the characteristics of a similar but high-aspect-ratio ( $AR = 20$ ) jet-flapped wing, Fig. 19b of Ref. 1 is added to this paper as Fig. 15. The effect of aspect ratio materializes in the following differences of the two figures:

- a) the strong increase in drag. It is illustrated by the vertical distance of corresponding lines in both figures for constant  $\Delta C_{LT}$ ,  $\theta$  or  $\alpha$  from the 100% thrust recovery slope line.
- b) the appreciable reduction in measured thrust ( $\Delta C_{TM}$ ). For instance, at  $\theta = 67^\circ$ ,  $\Delta C_{TM}$  is practically zero. In other words, the  $C_{\mu R}$  which is required to produce a desired lift is a thrust force annihilated by an equal but opposing drag force. A jet flap operated under such conditions would not at all contribute to the propulsive thrust.
- c) the straight portions of the  $\Delta C_{LT} = \text{constant}$  lines are no longer parallel to the 100% thrust recovery slope line. Their angle with the  $45^\circ$  line is a function of  $\Delta C_{LT}$ . The total drag along any of the straight-line portions decreases with increasing  $C_{\mu R}$ .
- d) the departure of the  $\Delta C_{LT} = \text{constant}$  lines from a straight line (where the operating line intersects) is more graduate with low-aspect-ratio jet-flapped wings. If  $\alpha$  is changed at constant  $\Delta C_{LT}$  and  $\theta$ , the total drag is always increasing in Fig. 14. In Fig. 15 (see  $\Delta C_{LT} = 3$  for instance), it initially decreases before it finally increases.
- e) the operating line is drawn as a straight line. This results from the vagueness of the location of the points which define where the  $\Delta C_{LT} = \text{constant}$  lines depart from straight lines. Actually, if this jet flap characteristics could be more comprehensive to include constant lift lines of up to  $\Delta C_{LT} = 7$ , the operating line should appear slightly curved downward.

## V. PERFORMANCE AND JET FLAP OPERATION

The jet flap is by its very nature a high-lift device. High lift can be obtained by a combination of jet sheet blowing with either jet deflection angle or angle of attack or both. A desired lift is produced most economically if the required rate of blowing and the inherent drag are the smallest values possible. Automatically, this defines the operating line as the line along which a jet-flapped wing should be operated.

### 5.1 Jet Flap Performance

For a lift of, say,  $\Delta C_{LT} = 3$ , point A (see Fig. 14) would be the proper operating point. If at constant  $\Delta C_{LT}$ , the jet deflection angle

is increased to  $\theta = 67^\circ$  (point B),  $C_{\mu R}$  is decreased from 0.84 to 0.64, but the total drag is somewhat increased (from 0.70 to 0.76). If at  $\Delta C_{LT} = 3$ , the jet deflection angle is reduced to, say,  $\theta = 37^\circ$ , the total drag (see point C) decreases to  $\Delta C_{DT} = 0.62$  (due to  $C_{D_i}$ ), but now the blowing rate is prohibitively high ( $C_{\mu R} = 2.3$ ).

If the angle of attack would be used to assist in the production of lift, Fig. 14 illustrates that under all circumstances  $\Delta C_{DT}$  would increase. This fact alone should in practice eliminate the use of  $\alpha$ . As will be shown more clearly in a later section, it is the total drag penalty commensurate with the high-lift production of jet-flapped wings, which is the most important and crucial parameter to watch.

The optimum jet deflection angle, as defined by the operating line, seems to be still of the order of  $\theta = 60^\circ$ . This value was previously found (Ref. 1) to apply for truly and quasi two-dimensional jet flapped wings. Note, that in the case of low-aspect-ratio jet flaps, the adherence to the optimum  $\theta$  is less critical because of the very gradual departure of the  $\Delta C_{LT} = \text{constant}$  lines from a straight line.

## 5.2 Most Economical Jet-Flap Operation

If a jet-flapped wing of the characteristics shown in Fig. 14 is to be incorporated in an aircraft design, economy of operation of the integrated lift and propulsive systems has to be considered. In other words, not only does a specific lift have to be produced at the smallest possible drag and blowing rate, but the losses in providing the propulsive thrust must be considered and be kept at a minimum.

From the viewpoint of lift production alone, lift could most economically be generated if the jet-flapped wing is operated along the operating line. For instance, for the specific lift of  $\Delta C_{LT} = 3$ , point A would specify the conditions for most economical operation. The jet flap's thrust  $\Delta C_{TM}$  at point A is 0.14, its drag ( $\Delta C_{DT}$ ) is 0.70, and the rate of blowing required for the production of  $\Delta C_{LT} = 3$  is  $C_{\mu L} = \Delta C_{TM} + \Delta C_{DT} = 0.84$ .

Theoretically, the rate of blowing ( $C_{\mu L}$ ) through the wing trailing edge slots, required solely for the production of the desired lift, may be smaller or equal to the optimum rate of blowing ( $C_{\mu E}$ ) which would result if the entire jet engine exhaust is expelled through the wing trailing edge slots. If  $C_{\mu L} < C_{\mu E}$ , there are two ways of handling that portion of the engine exhaust which is not required for jet flap-lift production but is crucial for the production of the propulsive thrust. One can either

- 1) eject the entire jet engine exhaust through the trailing edge slots (in this case, the operating point of the jet-flapped wing at  $\Delta C_{LT} = 3$ , for instance (see Fig. 14), would be shifted along the constant lift line from point A toward C,

depending on the magnitude of  $C_{\mu E}$ .

or

- 2) operate the jet-flapped wing at point A by feeding only the required  $C_{\mu L} = 0.84$  to the wing trailing edge slots (the uncommitted portion of the total engine exhaust ( $C_{\mu E} - C_{\mu L}$ ) is expelled in the conventional way through the exhaust nozzles of the jet engines).

The first alternative has the advantage of reducing the total drag on account of a reduction in  $CD_i'' = K^v \cdot \Delta C_{LT}^2 C_{\mu R}$  with  $C_{\mu R}$ . Its disadvantage is that the extremely large engine exhaust has to be ducted to the nozzle slots at the wing's trailing edge. Besides occupying valuable wing storage space, hot gas ducts pose mechanical problems. Furthermore, they impose frictional losses on the flow which may outweigh any gain by a reduction in total drag due to  $CD_i''$ . However, since both  $K^v$  and  $C_{\mu R}$  increase if a lower aspect ratio wing ( $AR = 3$ ) is used, the balance between  $CD_i''$  and the duct losses should be examined carefully.

Economically, the second alternative seems, at least theoretically, to be the more attractive one. During the take-off run along the ground and also in cruise, jet-flapped wings have nothing to offer economy-wise that conventional wings cannot offer. This is one reason why during both these operations, the airplane should be operated conventionally and the entire jet engine exhaust be expelled through the engine's propelling nozzles. They unquestionably produce propulsive thrust more efficiently than slot nozzles. Therefore, it is the instant of take-off from the ground that the jet-flap system should be put into operation and a metered amount of either hot jet engine exhaust or secondary (bypass) air be ejected through the wing trailing edge slots. The metered mass flow is just that amount which is required to furnish the desired jet flap lift.

The advantages of this scheme are obvious. Ducts can be smaller and thus dimensioned for low duct flow velocities and frictional losses. Rates of blowing are small enough to reduce the mechanical problems encountered in the deflection of large and fast-moving mass flows of hot gases. During cruise, the 2 to 5% loss in propulsive thrust due to duct and slot nozzle losses is avoided.

Whether in practice  $C_{\mu L}$  is smaller or equal to  $C_{\mu E}$  depends primarily upon the extent the high lift potential of jet-flapped wings is used and upon the mission requirements of the aircraft in question (rate of climb, cruising and top speed, etc.). In the following section, this point is discussed further.

### 5.3 The Jet-Flapped Wing and STOL

The aircraft chosen to subsequently demonstrate the potential of the jet flap for STOL application demands magnitudes of lift and rate of blowing which are far beyond the experimental ranges investigated in Ref. 2, and presented in the jet flap characteristics of Fig. 14. Because of this lack of experimental evidence, the following discussion is qualitative rather than quantitative.

If one divides the take-off and cruising thrust data of fighter aircraft, bombers, airliners, and trainers by the  $\rho/2 V^2$  at the instant of take-off from the ground and at cruise respectively, the resulting thrust coefficients were found to group around these values:

$$C_{\mu T} = 0.5 \quad (\text{take-off})$$

$$C_{\mu C} = 0.025 \quad (\text{cruise})$$

Let us consider now an airliner which at distance  $x$  takes off the ground with a  $C_{\mu T} = 0.5$ . This airliner is to be converted into a STOL aircraft by means of the jet flap principle, and its conventional take-off distance  $x$  is to be shortened to  $x/6$ . Weight and propulsive thrust are assumed to be the same for both aircraft. Since at take-off the lift acting on both aircraft must be the same, the relationship

$$C'_L \frac{\rho}{2} V_T'^2 = C_{LT} \frac{\rho}{2} V_T^2 = C_{LT} \frac{\rho}{2} \frac{V_T^2}{6} \quad (5.1)$$

holds assuming constant acceleration during the ground run. From Eq. 5.1, it then follows that  $C_{LT} = 6 C'_L$ . If  $C'_L$  for the conventional airliner at take-off is assumed to be 1.2,  $C_{LT}$  becomes 7.2. Similarly,  $C_{\mu T} = 0.5$  becomes  $C_{\mu} = 6 C_{\mu T} = 3$ .

In Ref. 1, it was demonstrated that with an  $AR \approx 20$  pure jet-flapped wing at  $\theta = 60^\circ$ ,  $\alpha = 0^\circ$ , and  $C_{\mu} = 3$ , a lift of  $\Delta C_{LT} = C_{LT} = 6.15$  only could be obtained. In order to provide the required take-off lift at  $\Delta C_{LT} = 7.2$ , either the engine thrust would have to be increased by 37% (to raise  $C_{\mu}$  from 3 to 4.1) or a jet-flapped wing which under similar conditions produces a higher lift than that of the pure jet flap has to be employed. Such jet-flapped wings are those equipped with shrouds or jet control flaps. They produce higher lifts on account of larger  $K$  values (see Eq. 3.5). For the pure jet flap,  $K$  was 4.1, whereas  $K$  values for jet-flapped wings with jet control flaps were found to be as high as 5.2. At  $AR \approx 20$ , a jet-flapped wing of  $K = 4.8$ ,  $\theta = 60^\circ$ ,  $\alpha = 0^\circ$ , and  $C_{\mu} = 3$  would be able to furnish the desired lift of  $\Delta C_{LT} = 7.2$  without any increase in engine thrust.

This high lift cannot be obtained without a simultaneous (induced) drag penalty, which comes into effect at that instant when the aircraft leaves the ground. The propulsive thrust available for climb (in comparison

with the conventional airliner) is reduced by an amount equivalent to this drag, resulting in a grossly reduced climb rate. In this case of an  $AR \approx 20$  jet-flapped wing, the propulsive thrust at the instant of take-off is only about half the thrust produced by the jet engines. Of course, things get worse with operational (low-aspect-ratio) jet-flapped wings. It will be shown next that the jet-flapped wing of Ref. 2 ( $AR = 6$ ) is not able to lift the converted airliner off the ground at 1/6 of the conventional take-off distance. This is due to the fact that the entire engine exhaust ( $C_{\mu} = 3$ ) at the take-off point is not large enough to satisfy the blowing rate ( $C_{\mu L}$ ) required to produce the desired lift of  $\Delta C_{LT} = 7.2$ .

If we use the  $AR = 6$  jet-flapped wing of Ref. 2 (see Fig. 14) at  $\theta = 55^\circ$  and  $\alpha = 0^\circ$ , we can calculate  $\Delta C_{DT_0}$  from Eq. 3.11 as

$$\Delta C_{DT_0} = 0.0833 \cdot \Delta C_{LT}^2 = 4.33 \quad ,$$

and a  $\Delta C_{LT} = 7.2$  line could be added in Fig. 4 as a straight line parallel to the 100% thrust recovery slope line. This line would be a line along which  $\Delta C_{DT_0} = \text{constant} = 4.33$ . The real  $\Delta C_{LT} = 7.2$  line can be found by subtracting  $C_{D_i}'' = 0.00464 \cdot \Delta C_{LT}^2 \cdot C_{\mu L}$  from  $\Delta C_{DT_0}$  at  $\theta = 55^\circ$ . To do this, we need to know  $C_{\mu L}$ , which we obtain from

$$C_{\mu L} = \frac{\Delta C_{DT_0}}{C_1 \sin^2 55} = 7.75 \quad .$$

Then

$$\Delta C_{D_i}'' = 0.00464 \cdot \Delta C_{LT}^2 \cdot 7.75 = 1.87$$

and

$$\Delta C_{DT} = \Delta C_{DT_0} - \Delta C_{D_i}'' = 4.33 - 1.87 = 2.46 \quad .$$

We see that the required  $C_{\mu L} = 7.75$  and that the available rate of blowing is only  $C_{\mu} = 3$ . To get the jet flap airliner off the ground, the thrust of the engines would have to be raised in the ratio of  $7.75/3 = 2.58$ . If this is done, the entire jet engine exhaust has to be ejected through the nozzle slots at the wing trailing edge. The propulsive thrust is thus produced exclusively by the jet flap. Its magnitude at the instant of take-off from the ground and during the climb is

$$C_T = C_{\mu L} - \Delta C_{DT} = 7.75 - 2.46 = 5.29 \quad .$$

This means an approximately 75% increase in propulsive thrust for climb in comparison with the conventional airliner ( $C_{\mu} = 3$ ). Furthermore, due to the increased thrust of the jet engines, the take-off speed is achieved in a still shorter take-off ground run, the actual distance being

$$\frac{x}{6 \cdot 2.58} = \frac{x}{15.5} \quad .$$

This turns the jet-flap version of the airliner into a potential STOL aircraft.

In order to be able to compare the jet flap version with the conventional airliner on an equal footing, let us equip also the conventional airliner with similar, more powerful jet engines. Both aircraft would equally accelerate during the take-off run up to the point  $x/15.5$ , at which the jet flap version becomes airborne. The conventional airliner reaches its take-off speed now at  $x/2.58$  or at a take-off distance of 6 times that of the jet flap version. During climb, the conventional airliner is superior in get-away speed and rate of climb due to higher initial take-off speed and propulsive thrust (less drag). Finally, at cruise both aircraft should be equivalent except for the higher losses accrued in the production of the propulsive thrust with the jet flap version, provided that the engine exhaust is ejected through the slot nozzles at the wing's trailing edge.

#### 5.4 Integration of the Lifting and Propulsive Systems

In the early days of the jet flap, H. Constant observed that "the propulsive jet of a modern aircraft, being a very powerful physical entity, should be one hundred per cent combined with the wing in flight near the ground". In other words, Constant suggested, at least for take-off, the complete integration of the propulsive system of a jet aircraft with its lifting system. In practice, this would mean that during take-off the entire jet engine exhaust is to be ejected through the slot nozzles at the wing's trailing edge.

It appears that when full use is made of the jet flap's high lift potential (in STOL application for instance), blowing rates for the production of the extremely high lift coefficients required make it necessary to expell the entire engine exhaust through the slot nozzles (see prev. Sec.). Over this portion of a flight mission, complete integration of the propulsive and lifting systems seems to evolve naturally. It stands to reason that the mechanical complexity of such an integrated system would eliminate the "luxury" of the conventional system as a standby for cruise, in spite of some undeniable advantages which it has to offer.

Let us assume now that for any special reason the jet engine thrust (and exhaust mass flow) is larger than that required for lift production at the slot nozzles. Theoretically, in this case, the surplus mass flow could be ejected either also through the slot nozzles or, if technically feasible, through conventional exhaust nozzles. Both possibilities, disregarding any mechanical problems which may refute either one, were discussed and evaluated in a previous section. Undoubtedly, if the total thrust is supplied by a number of small jet engines immersed in the wing, the added feature of a lower total drag (due to the larger  $\Delta C_{Di}$  with  $C_{\mu L}$ ) makes the integrated system still more attractive. If  $C_{\mu E} > C_{\mu L}$  in an integrated system, the jet flap could be operated (due to the higher  $C_{\mu L}$ ) at a lower jet deflection angle than that suggested by the intersection of the operating line with the  $\Delta C_{LT} = \text{constant}$  line for the desired lift. A smaller jet deflection angle during take-off would reduce the propulsive thrust losses due to jet flap ground interference.

The angle of attack may have lost its usefulness in producing lift with jet flap aircraft.

### 5.5 Wind Tunnel Testing of Jet-Flapped Wings

It is one of the benefits of jet flap characteristics to clearly define the most economical range of jet-flap operation. Information outside this range (above the operating line) is of no direct practical significance, except if it concerns data obtained just above the operating line (say,  $\theta = 67^\circ$ ). In this way, existing jet flap characteristics may point the way to more purposeful jet flap testing and help in the accumulation of test data, all of which is practically useful. Such data are still very much needed. Perhaps it is even possible to streamline the test program in such a way as to furnish data which can directly be plotted in the form of jet flap characteristics. The following procedure may be helpful.

The jet-flapped wing to be tested (three-dimensional) is set up on a lift-drag (thrust) balance at  $\alpha = 0^\circ$ , the wind tunnel is running at a fixed speed, and the jet control flap is set at a specific angle. At zero blowing, the  $C'_L$  and  $C'_D$  are recorded. Then blowing is initiated and  $C_\mu$  is increased until a predetermined  $\Delta C_{LT} = C_{LT} - C'_L$  is reached. Then  $C_{TM}$  is recorded and  $\Delta C_{TM}$  is obtained from  $\Delta C_{TM} = C_{TM} + C'_D$ . These data provide the first experimental point on a  $\Delta C_{LT} = \text{constant}$  line in the prospective jet flap characteristics after  $C_\mu$  is calculated. Next, the jet deflection is changed, and the whole procedure is repeated for another test point on the same  $\Delta C_{LT} = \text{constant}$  line, etc.

## REFERENCES

1. Korbacher, G.K. Performance and Operation of Quasi Two-Dimensional Jet Flaps, UTIA Report No. 90, April, 1963, TRECOM Technical Report 63-58, Nov. 1963. Jour. AIAA, Vol. 2, No. 1, Jan. 1964.
2. Alexander, A. J.  
Williams, J. Wind Tunnel Experiments on a Rectangular Wing Jet Flap Model of Aspect Ratio 6, A. R. C. 22, 947, June, 1961.
3. Spence, D. A. A Treatment of the Jet Flap by Thin Aerofoil Theory, R. A. E. Rep. Aero. 2568, Nov. 1955.
4. Maskel, E. C.  
Spence, D. A. A Theory of the Jet Flap in Three Dimensions, R. A. E. Rep. Aero. 2612, Sept. 1958, Proc. Roy. Aero. Soc., Vol. 251, June, 1959.

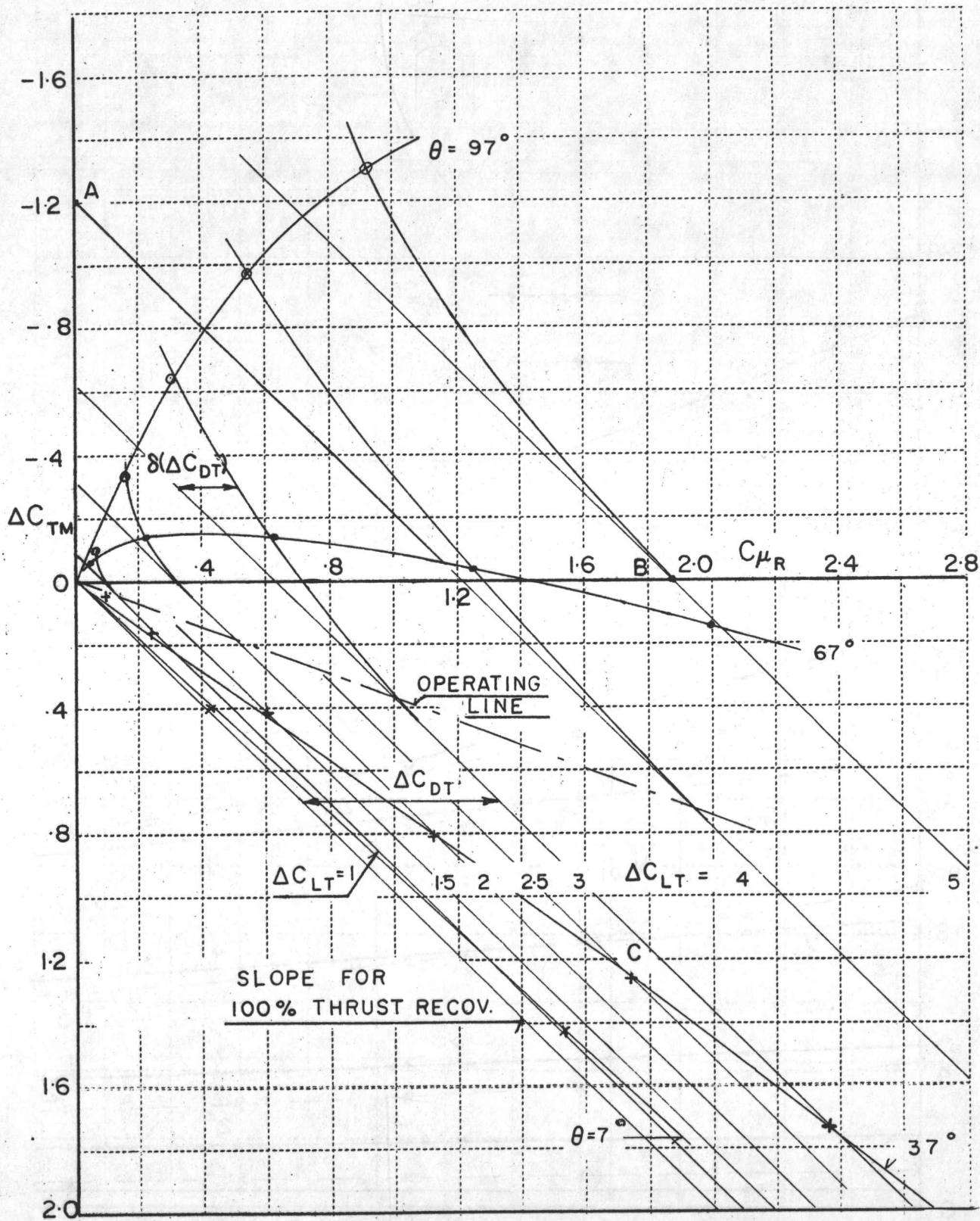


FIG. 1 IDEALIZED JET FLAP CHARACTERISTICS FOR A  $AR = 6$  JET FLAPPED WING AT ZERO ANGLE OF ATTACK (TEST DATA OF REF. 2).

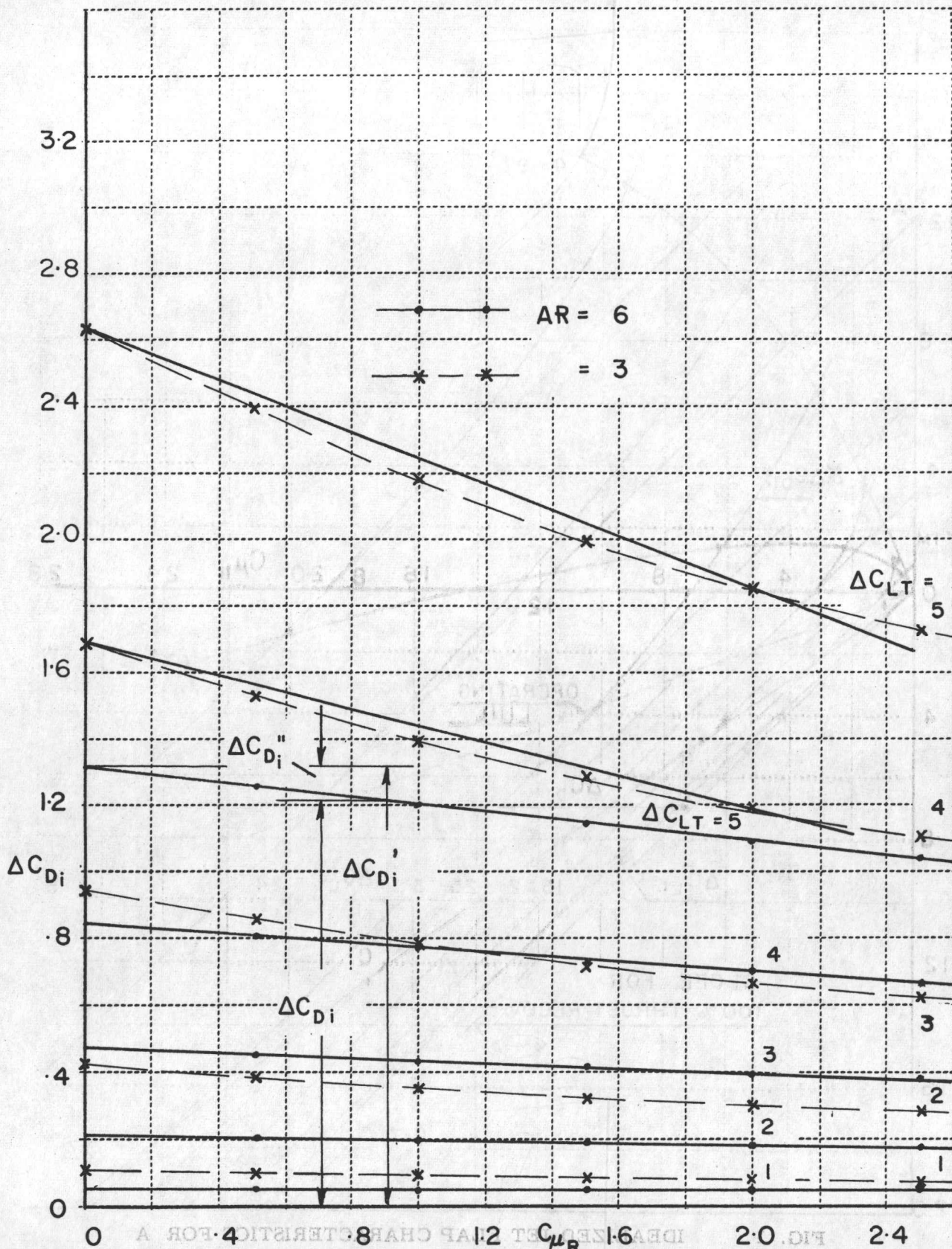


FIG. 2

CALCULATED INDUCED DRAG COMPONENTS,  $\Delta C'_{Di}$   
 DUE TO ASPECT RATIO,  $\Delta C''_{Di}$  DUE TO BLOWING  
 FOR VARIOUS LIFT VALUES AND TWO ASPECT RATIOS.

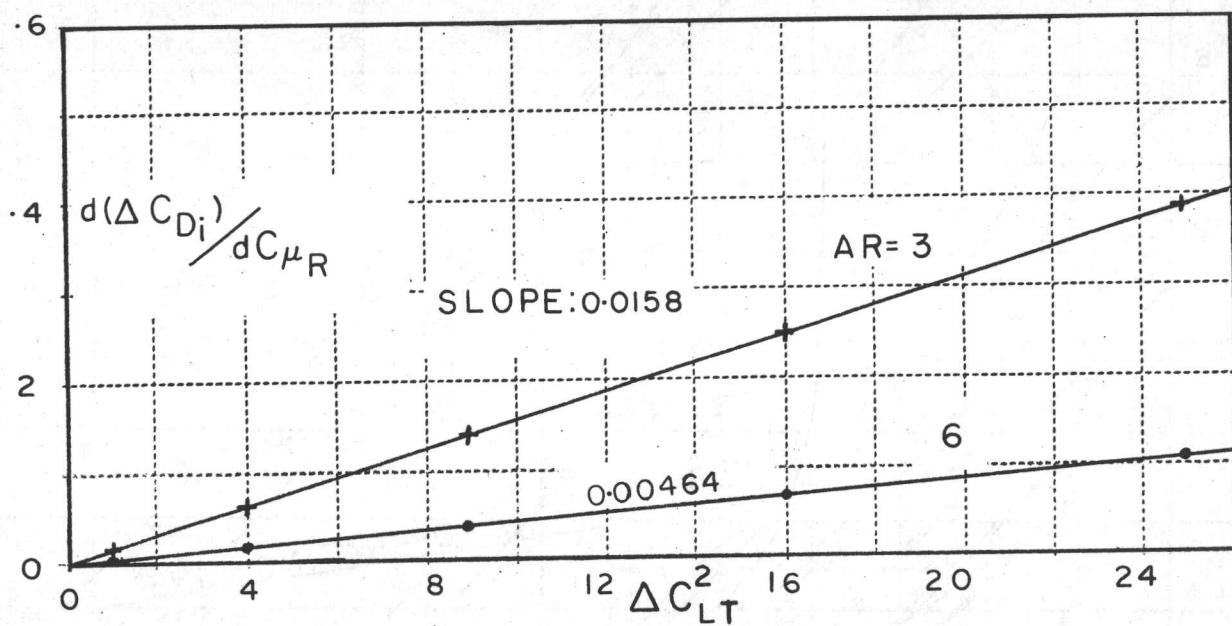


FIG. 3

THE SLOPE  $d(\Delta C_{Di})/d C_{\mu R}$  AS A FUNCTION OF  $\Delta C_{LT}^2$  FOR AR = 6 AND 3.

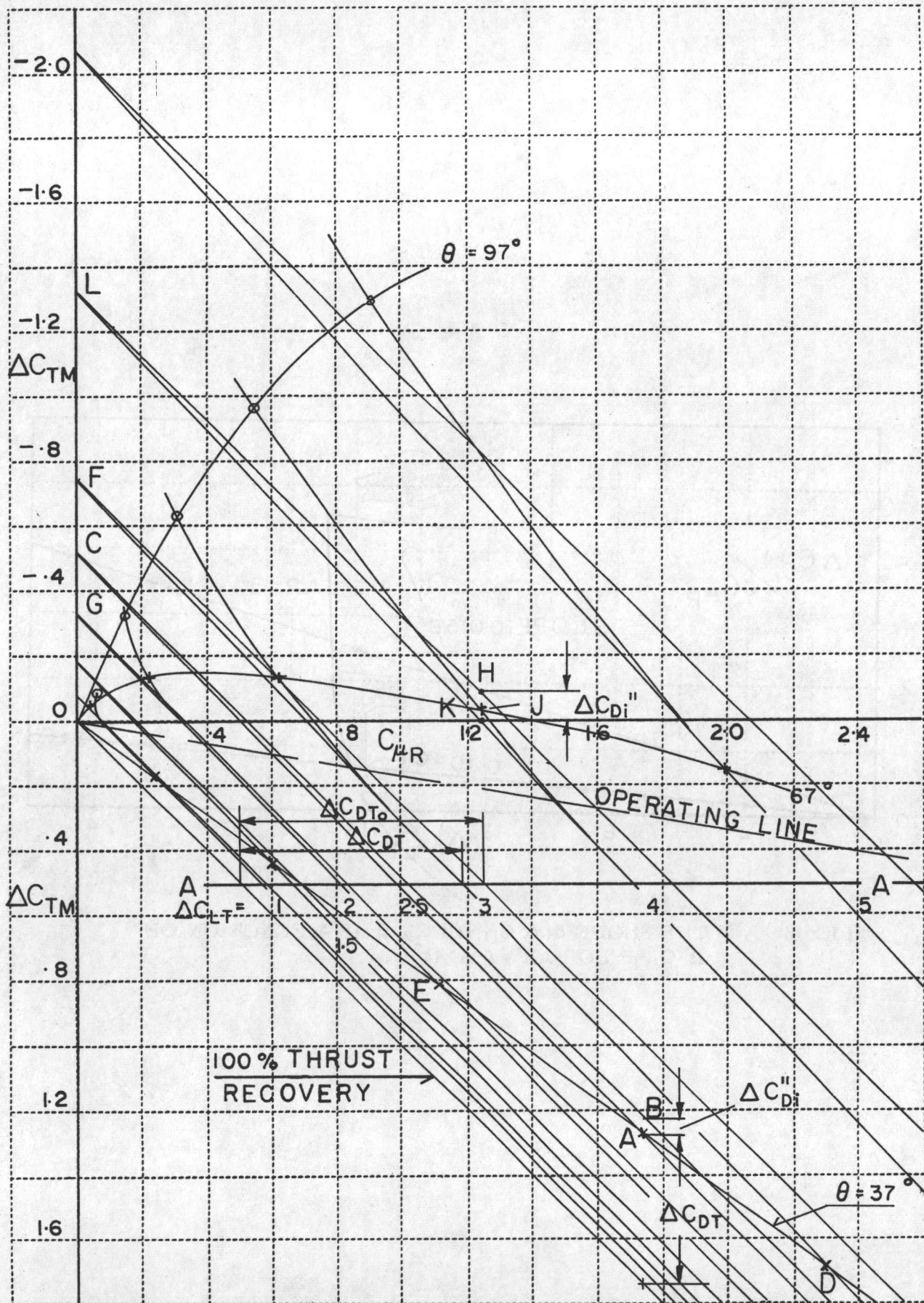


FIG. 4

JET FLAP CHARACTERISTICS FOR A  $AR = 6$  JET  
 FLAPPED WING AT ZERO ANGLE OF ATTACK  
 (TEST DATA OF REF. 2).

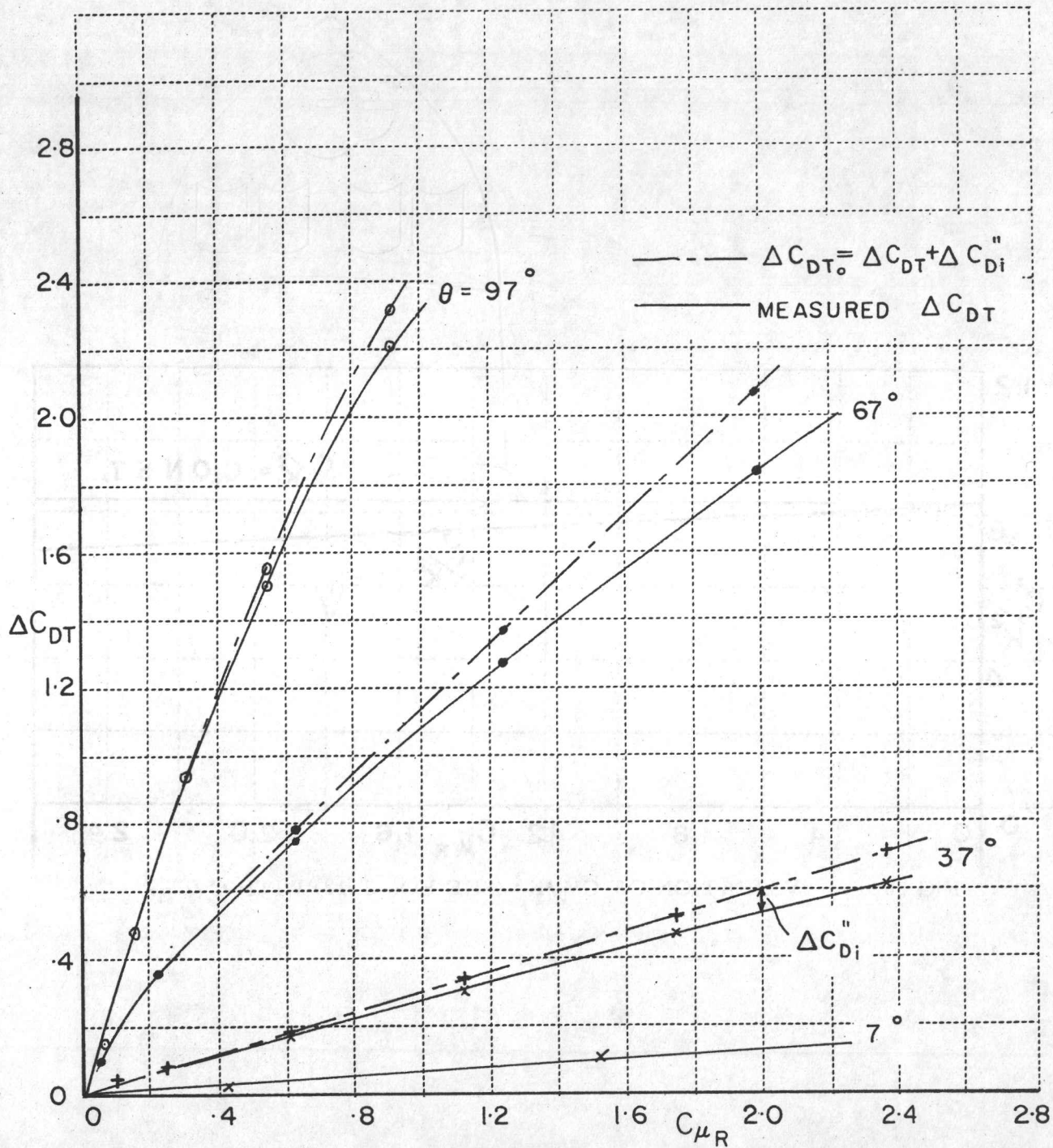


FIG. 5 VARIATION OF THE TOTAL DRAG AND THE INDUCED DRAG COMPONENT,  $\Delta C''_{Di}$  (SEE EQ. (3.10)) WITH  $C_{\mu R}$  AT VARIOUS JET DEFLECTION ANGLES.

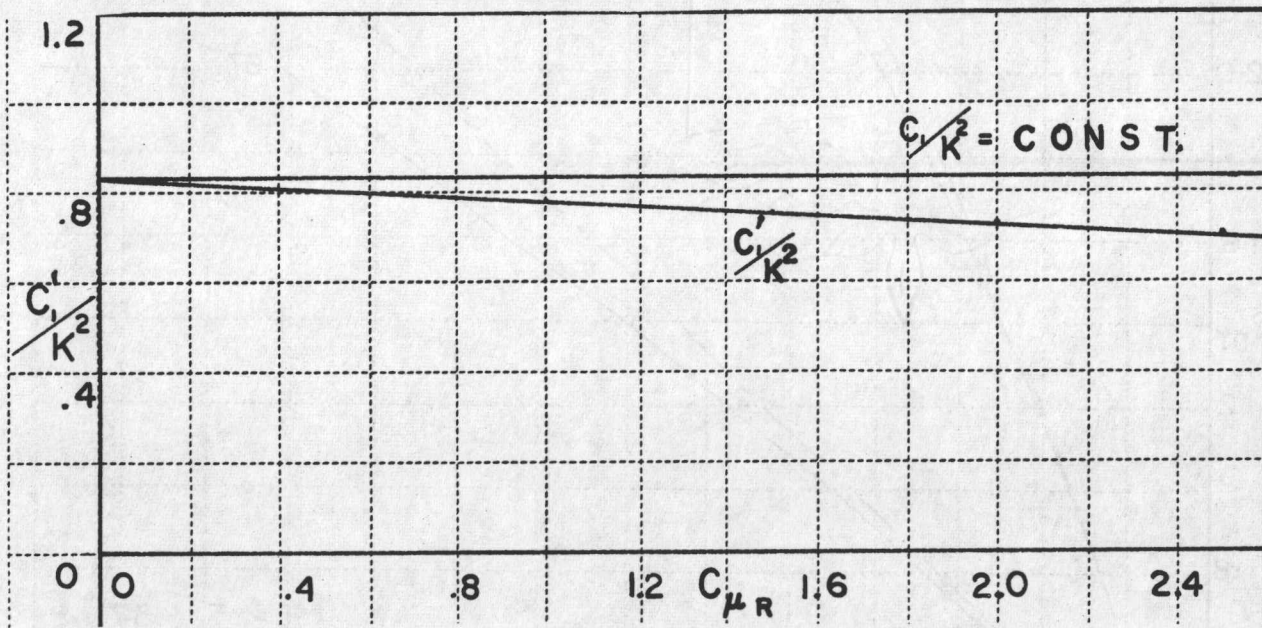


FIG. 6 VARIATION OF  $C'_1/K^2$  (SEE EQ. 3.12) WITH  $C\mu_R$ .

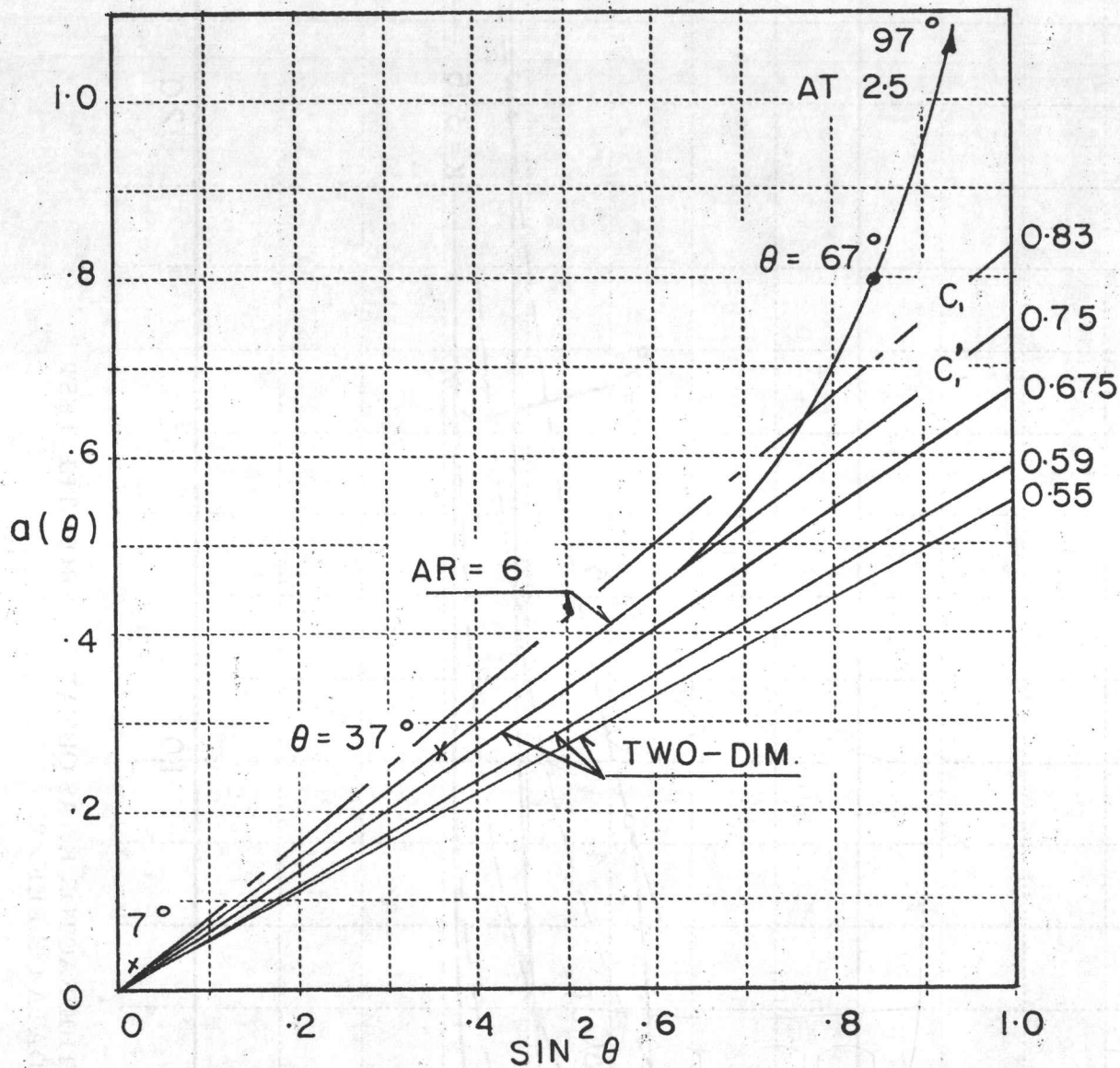


FIG. 7 THE SLOPES  $d a(\theta)/d \sin^2 \theta = C'_1$  and  $C_1$  FOR  $AR = 6$  AND FOR QUASI TWO-DIMENSIONAL JET FLAPPED WINGS.

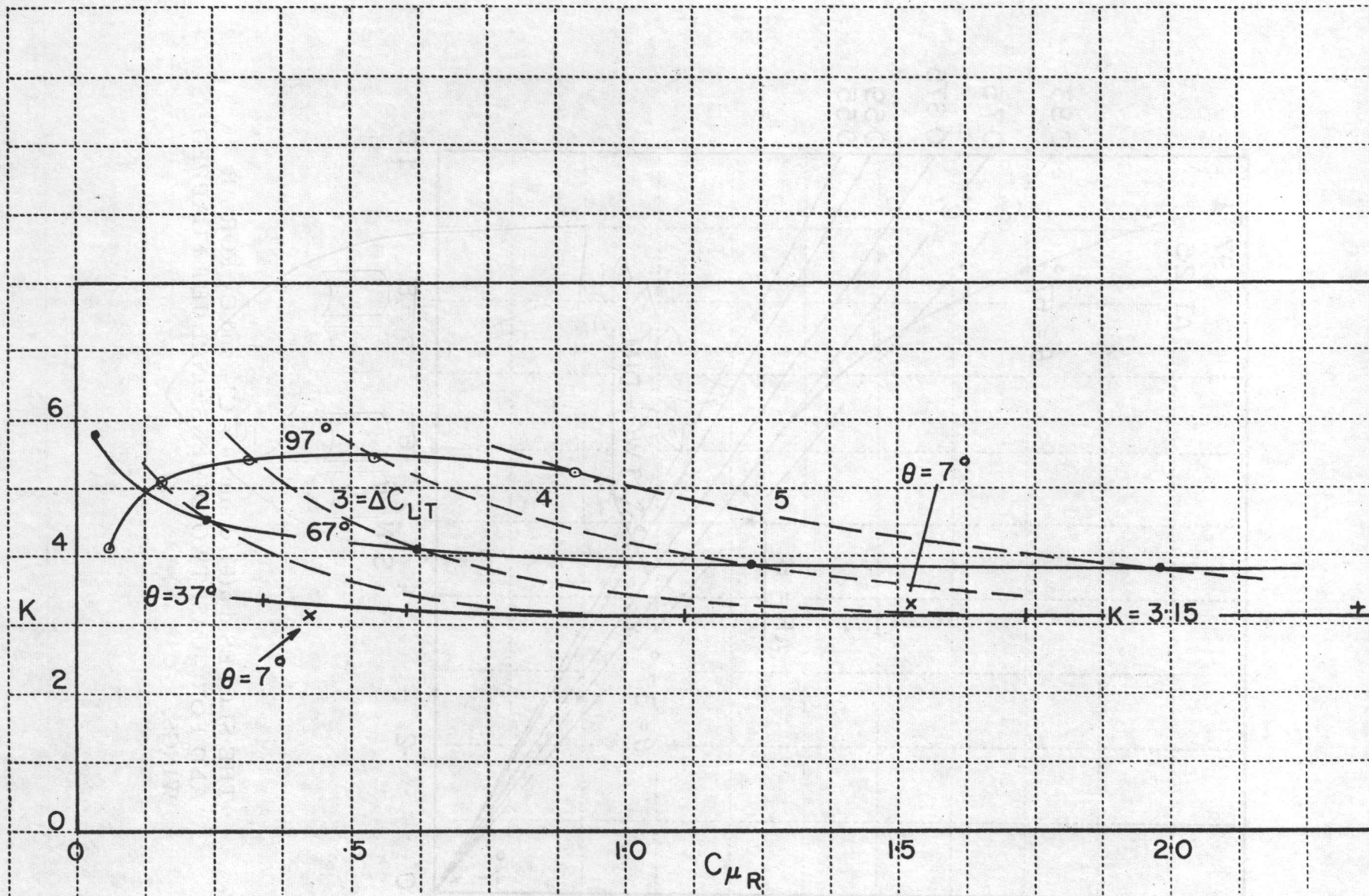


FIG. 8 THE FACTOR  $K$ , AS OBTAINED FROM THE TEST DATA OF REF. 2.

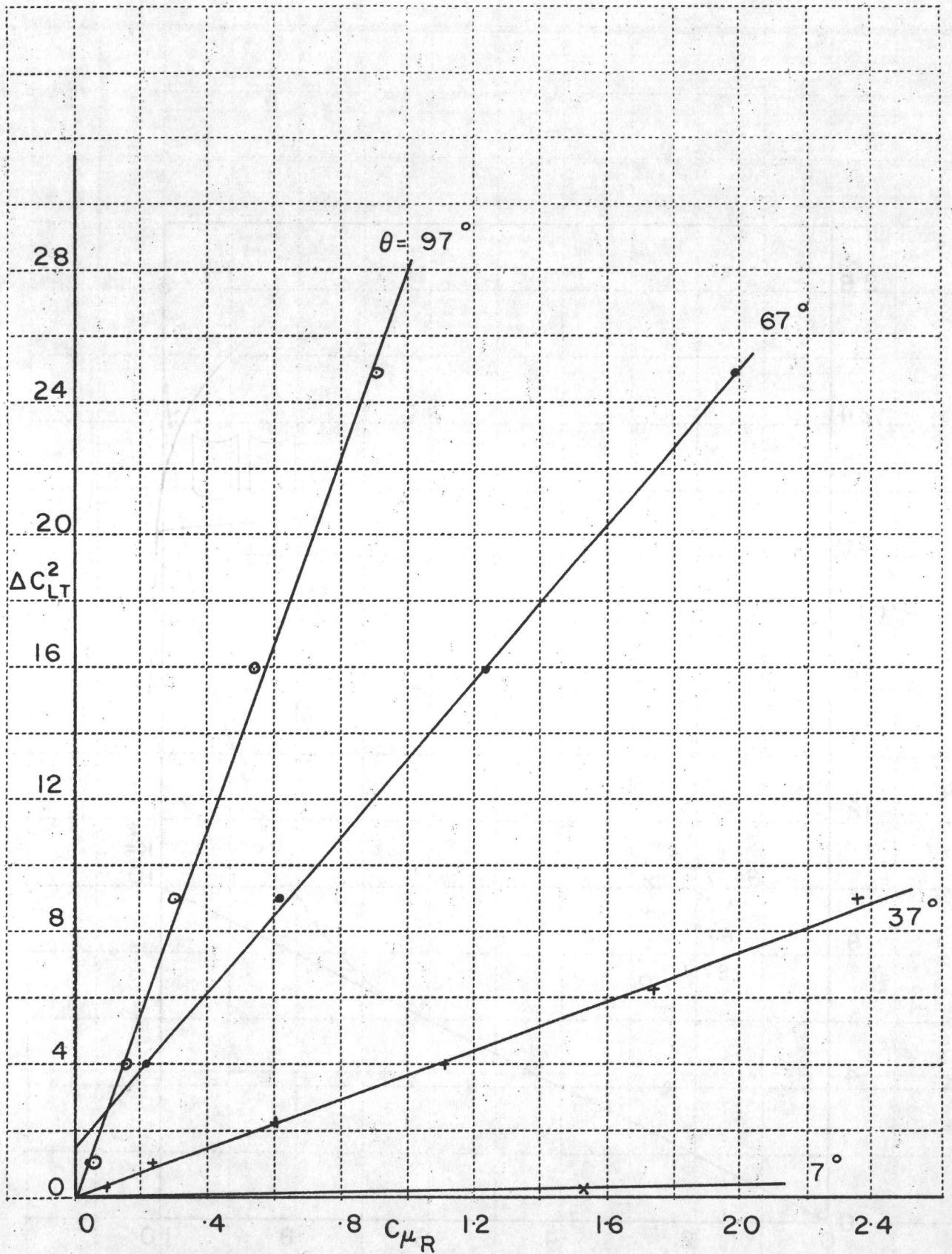


FIG. 9 THE LIFT SQUARED FOR VARIOUS JET DEFLECTION ANGLES AS A FUNCTION OF BLOWING (TEST DATA OF REF. 2).

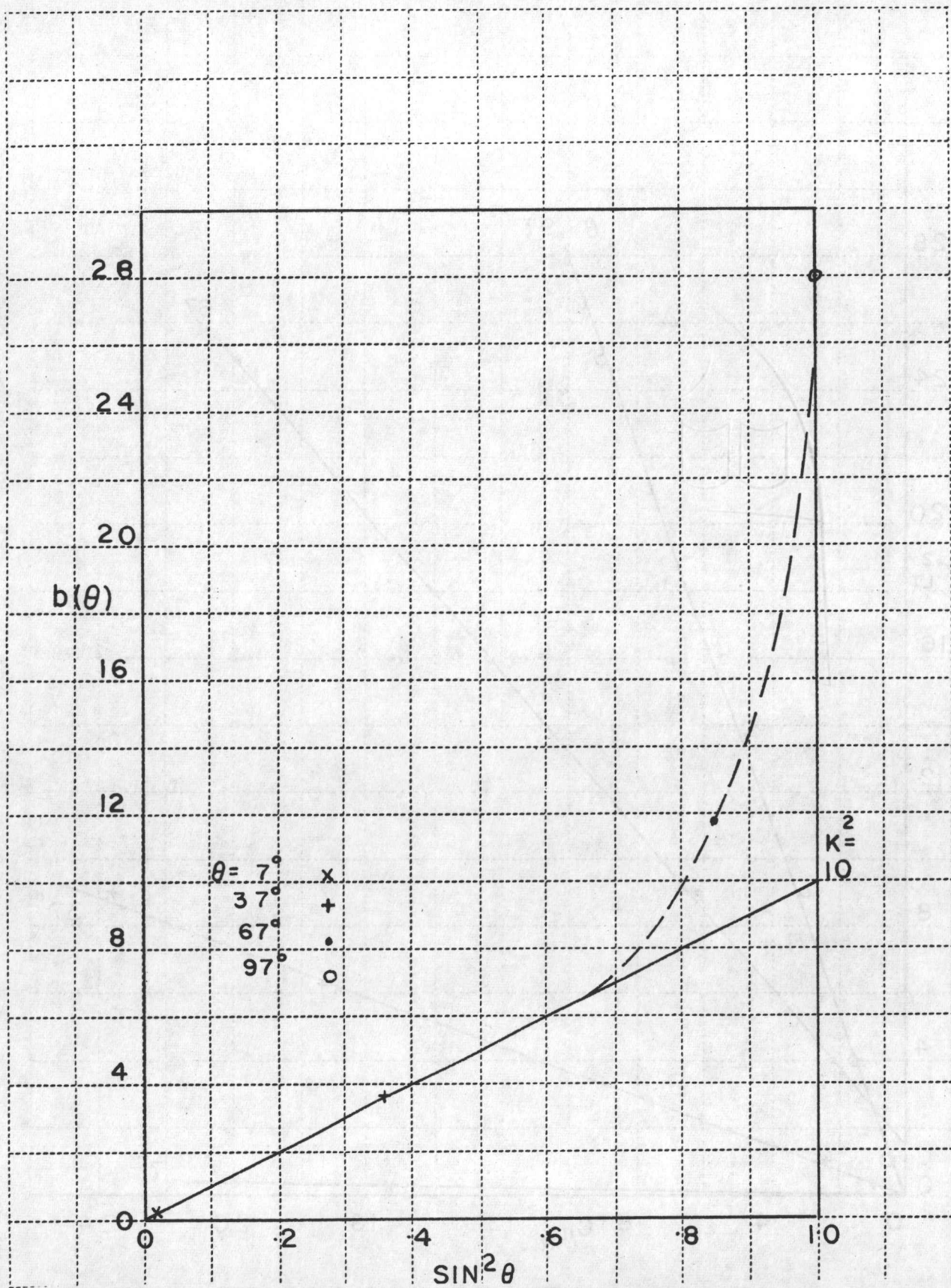


FIG. 10 THE SLOPE  $K^2 = d b(\theta) / d \sin^2 \theta$ , AS OBTAINED FROM THE TEST DATA OF REF. 2.

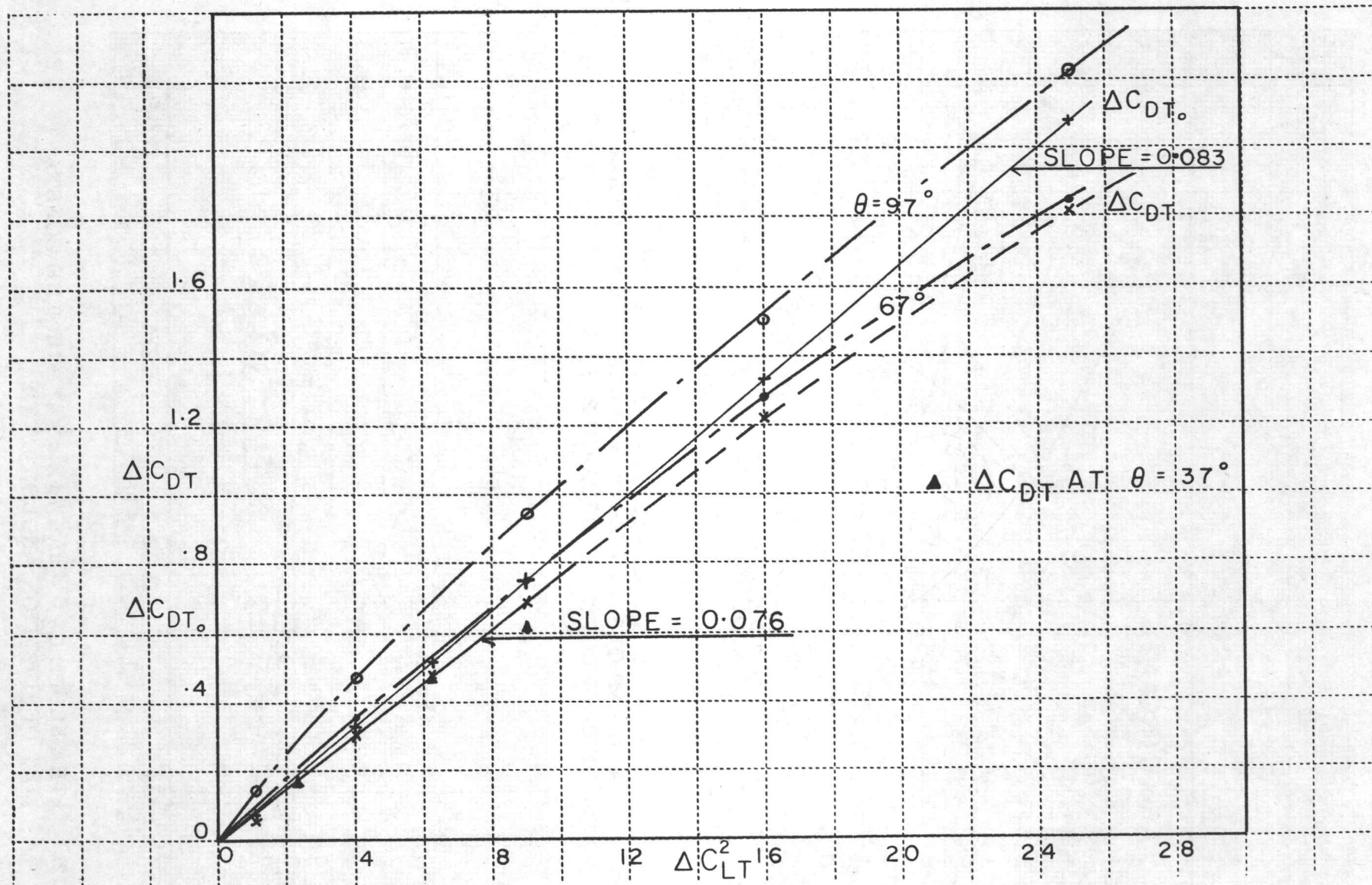


FIG. 11 THE SLOPE OF THE  $C_{DT}$  VERSUS  $C_{LT}^2$  CURVES FOR VARIOUS JET DEFLECTION ANGLES.

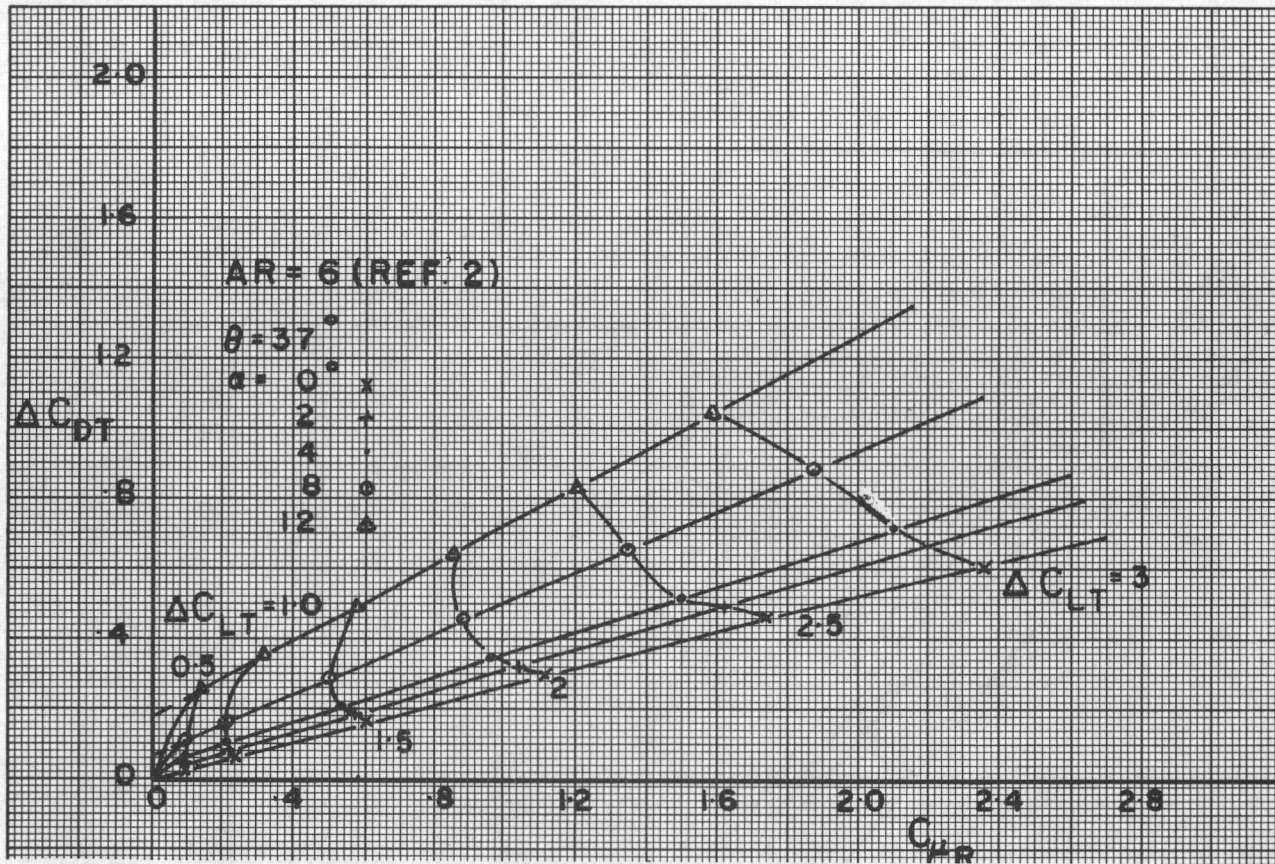


FIG. 12a THE TOTAL DRAG VARIATION AT A FIXED  $\theta = 37^\circ$  AND VARIOUS ANGLES OF ATTACK AS A FUNCTION OF BLOWING (TEST DATA OF REF. 2).

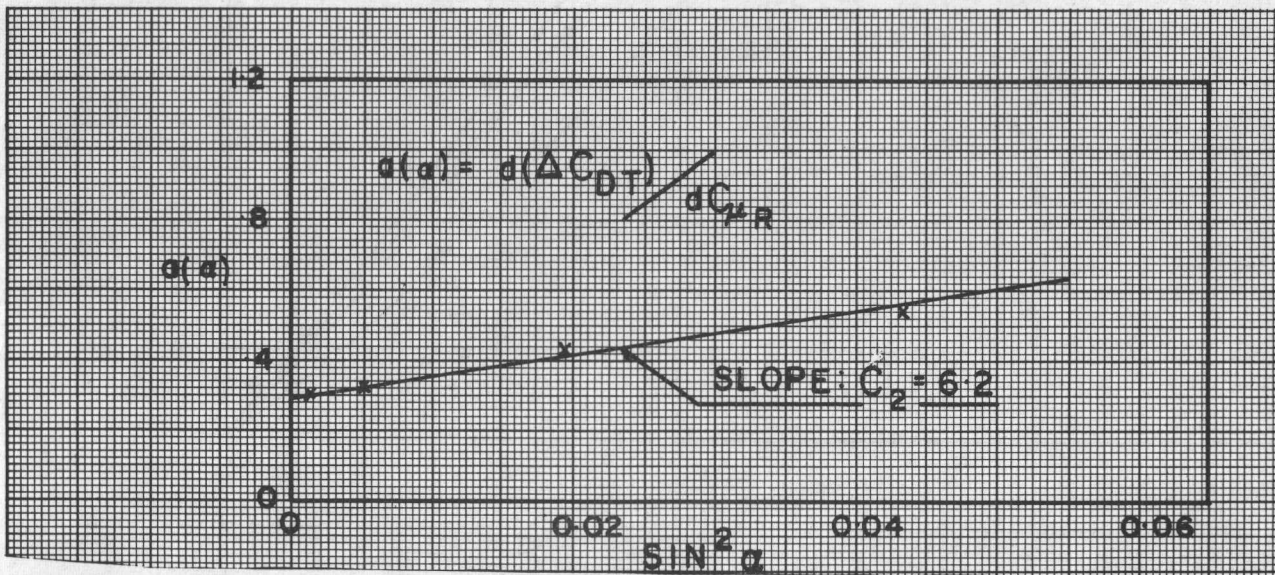


FIG. 12b THE SLOPE  $C_2 = d a(\alpha) / d \sin^2 \alpha$  FOR THE CONSTANT JET DEFLECTION ANGLE,  $\theta = 37^\circ$ .

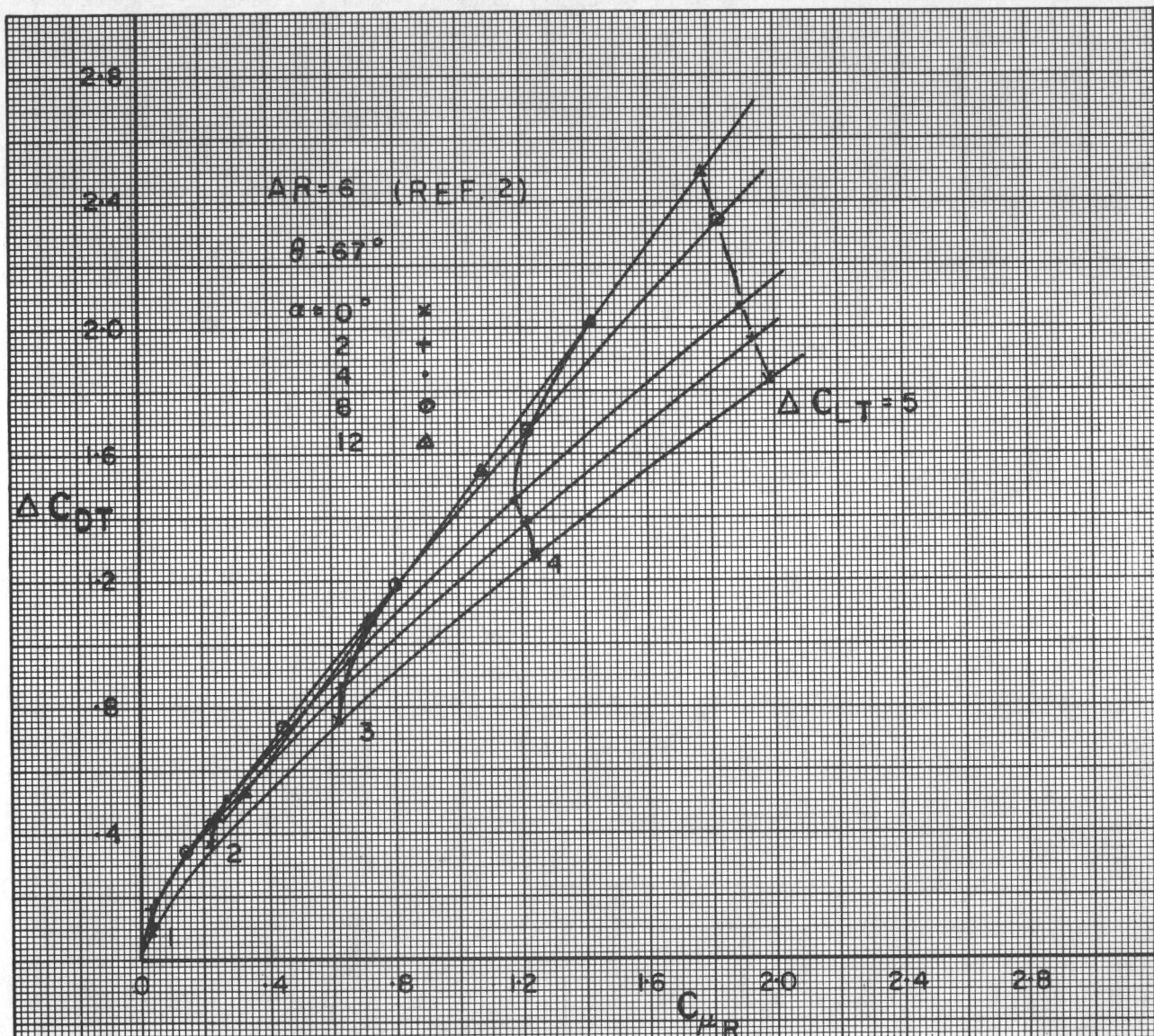


FIG 13 THE TOTAL DRAG VARIATION AT A FIXED  $\theta = 67^\circ$  AND VARIOUS ANGLES OF ATTACK AS A FUNCTION OF BLOWING (TEST DATA OF REF. 2).

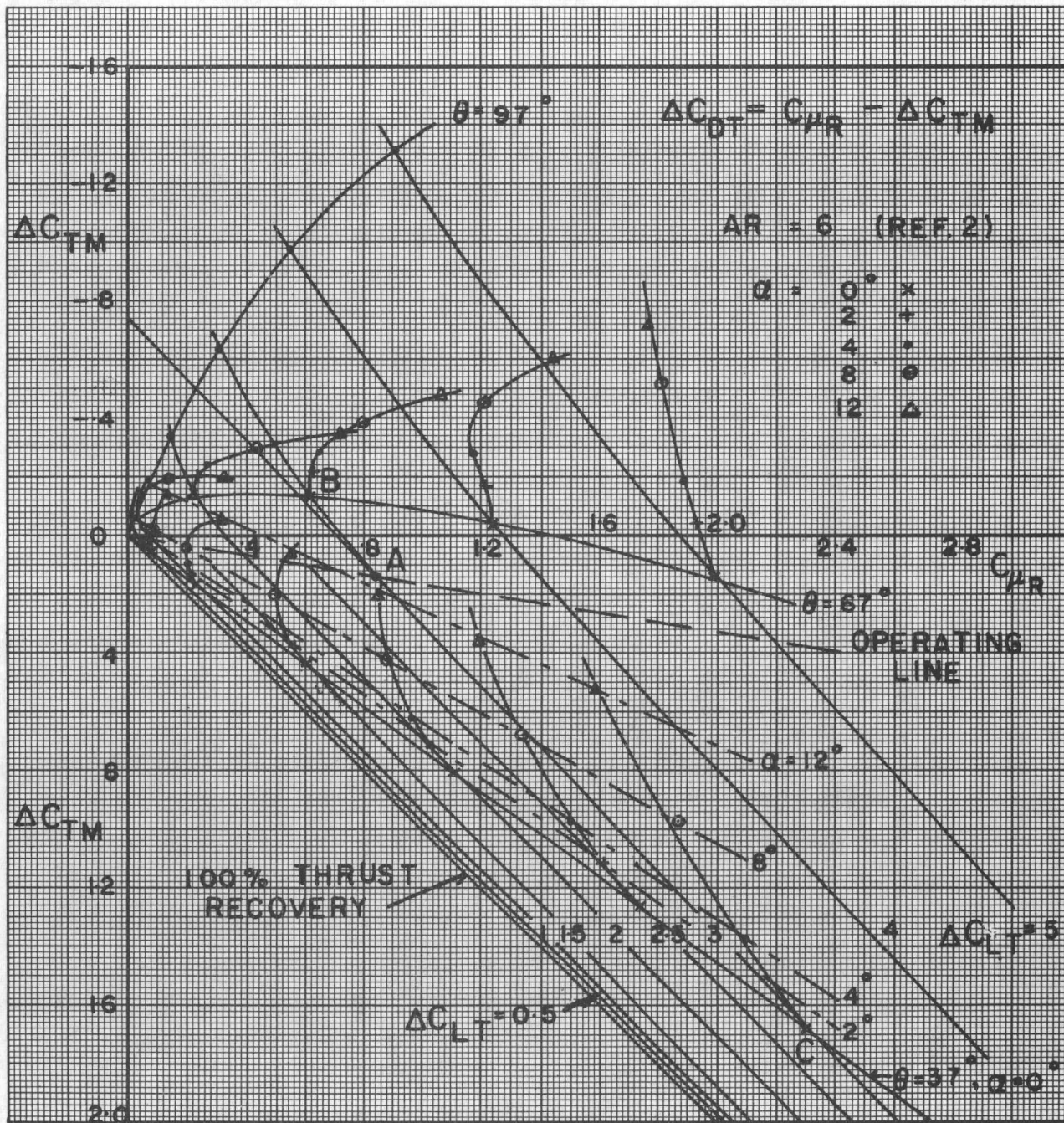


FIG. 14 JET FLAP CHARACTERISTICS FOR A AR = 6 JET FLAPPED WING AT VARIOUS ANGLES OF ATTACK FOR TWO FIXED JET DEFLECTION ANGLES ( $\theta = 37^\circ$  and  $67^\circ$ ) (TEST DATA OF REF. 2).

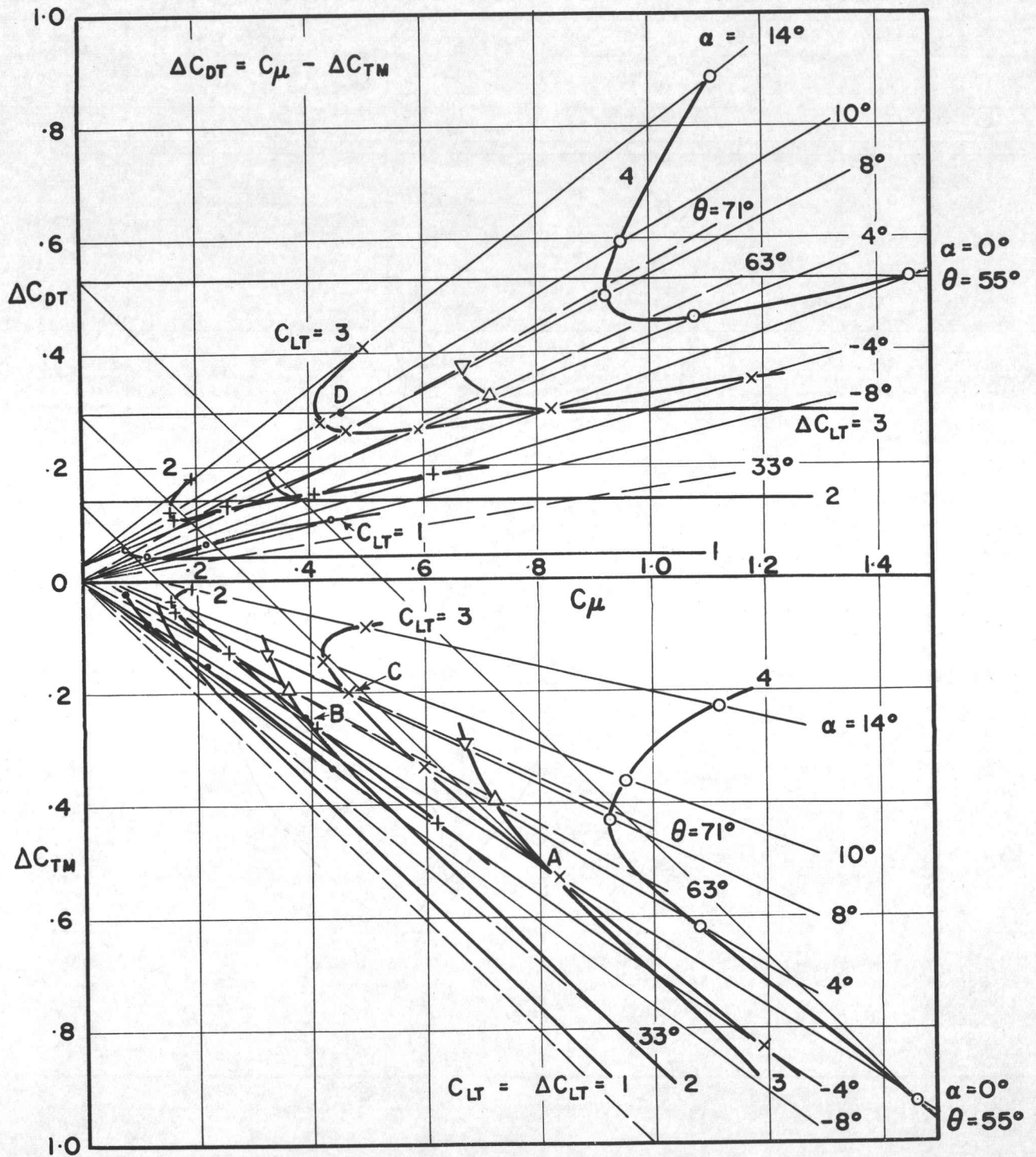
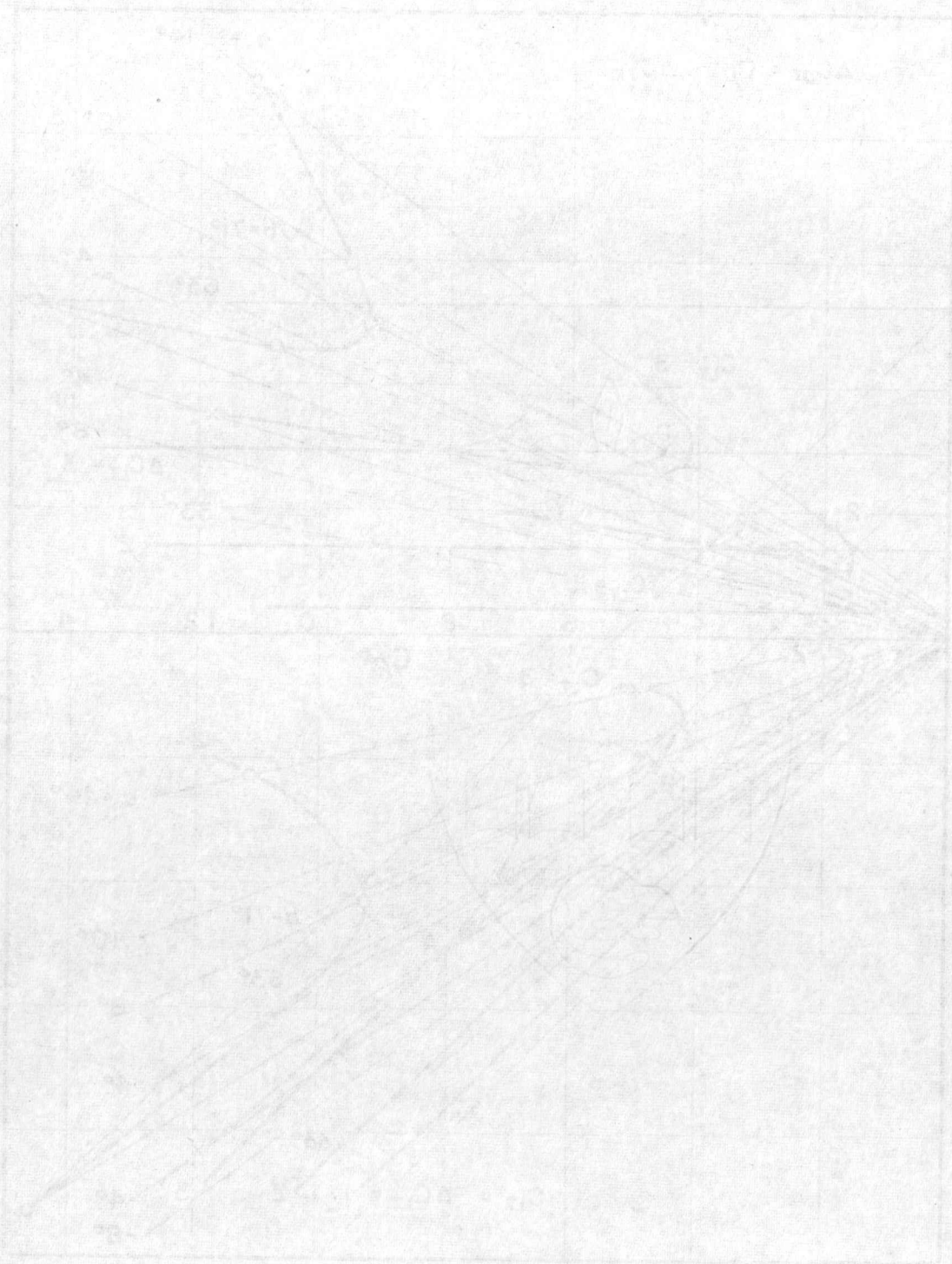


FIG. 15 JET FLAP CHARACTERISTICS FOR A AR = 20 JET FLAPPED WING AT A FIXED JET DEFLECTION ANGLE ( $\theta = 55^\circ$ ) AND VARIOUS ANGLES OF ATTACK.



THE UNIVERSITY OF CHICAGO  
LIBRARY

UTIAS REPORT NO. 97

Institute for Aerospace Studies, University of Toronto



Performance, Operation and Use of Low Aspect Ratio Jet Flapped Wings

G. K. Korbacher      May 1964      18 pages      15 figures

- |                    |                         |         |
|--------------------|-------------------------|---------|
| 1. Jet Flap        | 2. High Lift Devices    | 3. STOL |
| I. Korbacher, G.K. | II. UTIAS Report No. 97 |         |

The characteristics of a jet flapped wing of aspect ratio 6 are presented, discussed and evaluated for STOL application. Again, as for high aspect ratio (AR = 20) jet flapped wings, a range for most economical jet flap operation is well defined. The angle of attack as an efficient means of lift production loses its usefulness with low aspect ratio jet flapped wings, whereas the optimum jet deflection angle seems hardly affected ( $\theta \approx 55^\circ$ ). A most efficient jet flap application for STOL calls for a complete integration of the lifting and propulsive systems. In the range of most economical jet flap operation, semi-empirical relationships predict parameter changes accurately enough for practical purposes.

Available copies of this report are limited. Return this card to UTIAS, if you require a copy.

UTIAS REPORT NO. 97

Institute for Aerospace Studies, University of Toronto



Performance, Operation and Use of Low Aspect Ratio Jet Flapped Wings

G. K. Korbacher      May 1964      18 pages      15 figures

- |                    |                         |         |
|--------------------|-------------------------|---------|
| 1. Jet Flap        | 2. High Lift Devices    | 3. STOL |
| I. Korbacher, G.K. | II. UTIAS Report No. 97 |         |

The characteristics of a jet flapped wing of aspect ratio 6 are presented, discussed and evaluated for STOL application. Again, as for high aspect ratio (AR = 20) jet flapped wings, a range for most economical jet flap operation is well defined. The angle of attack as an efficient means of lift production loses its usefulness with low aspect ratio jet flapped wings, whereas the optimum jet deflection angle seems hardly affected ( $\theta \approx 55^\circ$ ). A most efficient jet flap application for STOL calls for a complete integration of the lifting and propulsive systems. In the range of most economical jet flap operation, semi-empirical relationships predict parameter changes accurately enough for practical purposes.

Available copies of this report are limited. Return this card to UTIAS, if you require a copy.

UTIAS REPORT NO. 97

Institute for Aerospace Studies, University of Toronto



Performance, Operation and Use of Low Aspect Ratio Jet Flapped Wings

G. K. Korbacher      May, 1964      18 pages      15 figures

- |                    |                         |         |
|--------------------|-------------------------|---------|
| 1. Jet Flap        | 2. High Lift Devices    | 3. STOL |
| I. Korbacher, G.K. | II. UTIAS Report No. 97 |         |

The characteristics of a jet flapped wing of aspect ratio 6 are presented, discussed and evaluated for STOL application. Again, as for high aspect ratio (AR = 20) jet flapped wings, a range for most economical jet flap operation is well defined. The angle of attack as an efficient means of lift production loses its usefulness with low aspect ratio jet flapped wings, whereas the optimum jet deflection angle seems hardly affected ( $\theta \approx 55^\circ$ ). A most efficient jet flap application for STOL calls for a complete integration of the lifting and propulsive systems. In the range of most economical jet flap operation, semi-empirical relationships predict parameter changes accurately enough for practical purposes.

Available copies of this report are limited. Return this card to UTIAS, if you require a copy.

UTIAS REPORT NO. 97

Institute for Aerospace Studies, University of Toronto



Performance, Operation and Use of Low Aspect Ratio Jet Flapped Wings

G. K. Korbacher      May 1964      18 pages      15 figures

- |                    |                         |         |
|--------------------|-------------------------|---------|
| 1. Jet Flap        | 2. High Lift Devices    | 3. STOL |
| I. Korbacher, G.K. | II. UTIAS Report No. 97 |         |

The characteristics of a jet flapped wing of aspect ratio 6 are presented, discussed and evaluated for STOL application. Again, as for high aspect ratio (AR = 20) jet flapped wings, a range for most economical jet flap operation is well defined. The angle of attack as an efficient means of lift production loses its usefulness with low aspect ratio jet flapped wings, whereas the optimum jet deflection angle seems hardly affected ( $\theta \approx 55^\circ$ ). A most efficient jet flap application for STOL calls for a complete integration of the lifting and propulsive systems. In the range of most economical jet flap operation, semi-empirical relationships predict parameter changes accurately enough for practical purposes.

Available copies of this report are limited. Return this card to UTIAS, if you require a copy.